

ICP/EXT-04-00172

Converting Simulated Sodium-Bearing Waste into a Single Solid Waste Form By Evaporation: Laboratory- and Pilot-Scale Test Results on Recycling Evaporator Overheads

*D. L. Griffith
R. J. Kirkham
L. G. Olson
W. D. St. Michel
S. J. Losinski*

**Idaho
Completion
Project**

Bechtel BWXT Idaho, LLC

January 2004

Converting Simulated Sodium-Bearing Waste into a Single Solid Waste Form By Evaporation: Laboratory- and Pilot-Scale Test Results on Recycling Evaporator Overheads

**Daniel L. Griffith
Robert J. Kirkham
Lonnie G. Olson
Whitney D. St. Michel
Sylvester J. Losinski**

January 2004

**Idaho Completion Project
Idaho Falls, Idaho 83415**

**Prepared for the
U.S. Department of Energy
Assistant Secretary for Environmental Management
Under DOE/NE Idaho Operations Office
Contract DE-AC07-99ID13727**

ABSTRACT

Conversion of Idaho National Engineering and Environmental Laboratory radioactive sodium-bearing waste into a single solid waste form by evaporation was demonstrated in both flask-scale and pilot-scale agitated thin film evaporator tests. A sodium-bearing waste simulant was adjusted to represent an evaporator feed in which the acid from the distillate is concentrated, neutralized, and recycled back through the evaporator. The advantage to this flowsheet is that a single remote-handled transuranic waste form is produced in the evaporator bottoms without the generation of any low-level mixed secondary waste. However, use of a recycle flowsheet in sodium-bearing waste evaporation results in a 50% increase in remote-handled transuranic volume in comparison to a non-recycle flowsheet.

SUMMARY

Conversion of surrogate Idaho National Engineering and Environmental Laboratory (INEEL) sodium-bearing waste (SBW) into a single solid waste form by evaporation was demonstrated in flask-scale and pilot-scale agitated thin film evaporator (ATFE) tests. The advantage to this flowsheet is that a single remote-handled transuranic (RH-TRU) waste form is produced without the generation of a secondary waste stream from the condensation of evaporator overheads (i.e., distillate).

Producing a single waste form in this manner requires that acid in the evaporator overheads be concentrated, neutralized, and recycled. This report presents results from the flask-scale and pilot-scale ATFE tests that were run to evaluate an “SBW with overhead recycle evaporation flowsheet.” Three different surrogate waste feeds were tested at the flask-scale including simulated waste feed compositions that would result from neutralizing the overheads with sodium, aluminum, or magnesium and blending this recycle stream with simulated SBW. The flask-scale tests were completed to identify appropriate mass reduction ratios for each of the three recycle flowsheets. Solid evaporator bottoms product characteristics, such as pourability, solidification capability, and product toughness (e.g. hardness, non-friable/monolithic), were evaluated for acceptability. This included an evaluation of the effects of overhead recycle on bottoms product characteristics. The SBW with aluminum and magnesium recycle flowsheets yielded bottom waste form products with acceptable characteristics. However, the SBW with sodium recycle flowsheet feed formed crystals in the evaporation flask and had to be concentrated more than the others to produce a solid bottoms waste form upon cooling. Based on the results of the flask-scale tests, only the aluminum and magnesium recycle feeds were tested in the pilot-scale ATFE.

ATFE pilot-scale tests yielded bottoms product with desirable characteristics for both of the simulated waste feeds tested. However, neutralizing with magnesium oxide would be the preferred choice for producing a single waste form with overhead recycle. The original concept of direct evaporation was based on the ability of aluminum nitrate to chemically bond with nine moles of water per mole of aluminum. However, magnesium nitrate performs at least as well. Both aluminum and magnesium nitrate will chemically bond three moles of water per mole of nitric acid neutralized. The main advantage of magnesium is that magnesium oxide readily dissolves and neutralizes evaporator overheads. No aluminum compound was identified that would dissolve as readily.

These tests demonstrated that SBW could be converted to a single solid RH-TRU waste form by evaporation/solidification with overheads neutralization and recycle, although processing issues may arise depending on the evaporation process selected.

ACKNOWLEDGMENTS

This work was performed for the U. S. Department of Energy's Idaho National Engineering and Environmental Laboratory High-Level Waste Program "SP4-SBW to WIPP" project under contract number DE-AC07-99ID13727. It meets, in part, the Idaho Completion Project's requirements for Project Baseline Initiative Performance Measure I.1a, Part 3.

We also wish to acknowledge and thank those who helped in any way with this study, including John McCray, Brett Olaveson, Vince Maio, Arlin Olson, Dave Macdonald, Richard Wood, Jeff Long, and the INTEC Analytical Laboratory Department.

CONTENTS

ABSTRACT.....	iii
SUMMARY	iv
ACKNOWLEDGMENTS	v
ACRONYMS.....	x
1. INTRODUCTION.....	1
1.1 Background	1
1.2 Purpose and Scope.....	2
1.3 Test Objectives	2
1.3.1 Material and Energy Balance	2
1.3.2 Control of Evaporator Bottoms Concentration.....	2
1.3.3 Fouling of Heating Surface	2
1.3.4 Plugging of Product Outlet.....	2
1.3.5 Waste Form Properties	2
1.3.6 Waste Form Critical Parameters Assessment.....	2
2. THEORY/EXPERIMENTAL APPROACH.....	3
2.1 Material and Energy Balance	6
2.1.1 Distillate Composition.....	6
2.1.2 Off-Gas Emissions	6
2.1.3 Overall Heat Transfer Rate.....	7
2.2 Control of Evaporator Bottoms Concentration.....	7
2.3 Fouling of Heating Surface	7
2.4 Plugging of Bottoms Outlet.....	7
2.5 Waste Form Properties	7
2.6 Waste Form Critical Parameters Assessment.....	7
2.6.1 Radiological Properties	8
2.6.2 Hydrogen Generation and Total Gas Limits	8
2.6.3 Chemical Compatibility	8
2.6.4 Corrosivity/Free Liquids	9
2.6.5 Ignitability	9

3.	EXPERIMENTAL SETUP	10
3.1	Evaporator Feed Preparation	10
3.1.1	Flask-Scale Tests	11
3.1.2	Pilot-Scale Tests	12
3.2	Experimental Apparatus	12
3.2.1	Flask-Scale Tests	12
3.2.2	Pilot-Scale Tests	15
3.3	Test Procedure	19
3.3.1	Flask-Scale Tests	19
3.3.2	Pilot-Scale Tests	20
4.	TEST RESULTS	22
4.1	Material and Energy Balance	22
4.1.1	Distillate Composition	22
4.1.2	Off-Gas Emissions	25
4.1.3	Overall Heat Transfer Rate	26
4.2	Control of Evaporator Bottoms Concentration	27
4.3	Fouling of Heating Surface	28
4.4	Plugging of Bottoms Discharge	29
4.5	Waste Form Properties	32
4.5.1	Flask-Scale Tests	32
4.5.2	Pilot-Scale Tests	33
4.6	Waste Form Critical Parameters Assessment	42
4.6.1	Radiological Properties	42
4.6.2	Hydrogen Generation and Total Gas Limits	43
4.6.3	Chemical Compatibility	44
4.6.4	Corrosivity/Free Liquids	45
4.6.5	Ignitability	47
5.	CONCLUSIONS	48
6.	RECOMMENDATIONS	50
7.	REFERENCES	51
	APPENDIX A, Analytical Results for Feed and Distillate Composition	53

FIGURES

1. Direct evaporation with acid recycle block flow diagram	3
2. Flask-scale test apparatus.....	14
3. Agitated thin film evaporator pilot plant	16
4. Evaporator rotor.....	17
5. Normal appearance inside the evaporator.....	17
6. Agitated thin film evaporator.....	18
7. Condensate discharge system	19
8. Acid feed fraction in distillate.....	22
9. Weight% mercury and chloride accumulated in the overheads for the sodium-neutralized recycle flowsheet	23
10. Weight% mercury and chloride accumulated in the overheads for the magnesium-neutralized recycle flowsheet	23
11. Weight% mercury and chloride accumulated in the overheads for the aluminum-neutralized recycle flowsheet	24
12. Conceptual graphic of the log-mean temperature difference used to calculate energy balance	27
13. Feed fraction evaporated versus bottoms temperature.....	28
14. Evaporator bottom discharge for the high aluminum feed at 54.7 wt% (a) and 62 wt% (b) and for the high magnesium feed at 54 wt% (c) and 61 wt% (d)	29
15. View of the AL-2 (62 wt%) bottoms leaving the timed discharge vessel	30
16. Evaporator rotor with buildup of bottoms	31
17. Inside evaporator vessel after discharge plugged	31
18. Thermocouples in first drum for the high aluminum feed and 54.7 wt% evaporated.....	35
19. Thermocouples in drum with high magnesium feed and 55 wt% evaporated	36
20. Photograph of solidified surface layer of Drum 1; aluminum recycle at 55% mass reduction.....	36
21. Photograph of solidified surface layer of Drum 3; magnesium recycle at 55% mass reduction	37
22. Cooling temperature profile for Drum 1	37
23. Cooling temperature profile for Drum 2	38

24. Cooling temperature profile for Drum 3	39
25. Cooling temperature profile for Drum 4	40
26. Drum headspace NO _x levels during cooling	44
27. Solidified product from SBW with magnesium-oxide-neutralized overheads pilot run – 62 wt% evaporated	46
27. Solidified product from SBW with aluminum-hydroxide-neutralized overheads pilot runs – 62 wt% evaporated	46

TABLES

1. Target feed composition calculations for SBW with recycled magnesium-oxide-neutralized overheads	4
2. Target feed composition calculations for SBW with recycled aluminum-hydroxide-neutralized overheads	5
3. Target feed compositions for flask- and pilot-scale tests	10
4. Actual flask-scale feed compositions	11
5. Actual pilot-scale feed compositions	13
6. Flask-scale test conditions	19
7. Test parameters for LCI Series 3 tests	20
8. Weight percent of each feed component that partitioned to the distillate	25
10. Calculated energy balance for each ATFE pilot-scale run	27
11. Waste form data for the flask-scale tests	32
12. Bottoms composition, in weight percent, for the ATFE pilot-scale runs	33
13. Volume reduction data for the pilot-scale runs	34
14. Physical drum dimensions before product loading and after solidification	41
15. Theoretical calculations to determine TRU activities	43
16. NO _x levels in headspace of cooled bottoms drums	45
17. Visual examination results of the experimental waste forms from flask-scale tests	46

ACRONYMS

ATFE	Agitated Thin Film Evaporator
DOE	Department of Energy
DOT	Department of Transportation
E/S	evaporation/solidification
INEEL	Idaho National Engineering and Environmental Laboratory
INTEC	Idaho Nuclear Technology and Engineering Center
LCI	LCI Corporation, Formerly Luwa Corporation
RH	remote-handled
SAR	Safety Analysis Report
SBW	sodium-bearing waste
TFF	Tank Farm Facility
TRU	transuranic
WIPP	Waste Isolation Pilot Plant

Converting Simulated Sodium-Bearing Waste into a Single Solid Waste Form By Evaporation: Laboratory- and Pilot-Scale Test Results on Recycling Evaporator Overheads

1. INTRODUCTION

Section 1 presents the background to the tests, gives the purpose and scope, and lists the objectives to the tests.

1.1 Background

As part of a Settlement Agreement between the Department of Energy (DOE) and the State of Idaho,^a the radioactive-waste-containing Tank Farm Facility (TFF) tanks at the Idaho National Engineering and Environmental Laboratory's (INEEL's) Idaho Nuclear Technology and Engineering Center (INTEC) must be taken out of service by December 31, 2012. One requirement in meeting this critical milestone is the removal and treatment of approximately 3,406,770 L (900,000 gal) of liquid radioactive sodium-bearing waste (SBW) and 302,824 L (80,000 gal) of tank heel solids material remaining in the TFF.

SBW is acidic with high concentrations of dissolved sodium and nitrate. As a byproduct of former indirect fuel reprocessing operations at INTEC, its chief sources were from solvent cleanup and equipment decontamination. Currently, the liquid SBW is stored in three 1,135,590-L (300,000-gal) capacity underground storage tanks at the TFF. These tanks are designated WM-180, WM-188, and WM-189.

The tank heel solids consist of the residual material left in tanks that have been emptied by normal means. The tank heel solids are a sludge-consistency, composed of small amounts of precipitate, undissolved material from fuel reprocessing, and dirt from decontamination operations. Sludge heels remain in Tanks WM-181 and WM-187.

One alternative being considered for SBW treatment is direct evaporation (E) followed by solidification(s) of the concentrated bottoms residue (E/S). E/S treatment involves the volume and mass reduction of the liquid SBW (mixed with heel solids) via evaporation, with subsequent cooling of the evaporator bottoms to form a solid waste form. The solid concentrate would be classified as remote-handled (RH) transuranic (TRU) waste and could potentially be disposed of at the DOE's Waste Isolation Pilot Plant (WIPP) with no additional treatment.

Direct E/S was successfully demonstrated at the flask-scale using simulated and actual SBW.^{1,2,3} A follow-on engineering study determined that an agitated thin film evaporator (ATFE) process was the best choice for testing to validate large-scale, continuous, SBW solidification by direct evaporation.⁴ Subsequent testing of a simulated SBW, containing no solids, was successfully completed in a series of tests, both at the flask-scale and in a pilot-scale ATFE.⁵ A second series of flask-scale and ATFE pilot-scale tests was completed to demonstrate the feasibility of co-processing the SBW and the tank heel solids.⁶

a. Consent Order and Settlement Agreement between the U. S. Department of Energy and the State of Idaho Regarding Spent Fuel and Nuclear Waste Issues, October 17, 1995.

1.2 Purpose and Scope

The main purpose for this study was to evaluate the evaporator overhead composition versus evaporation bottoms product concentration, and characteristics, as well as the continuous processing of simulated SBW with overheads recycle feeds that contain higher concentrations of magnesium, aluminum, or sodium and lower concentrations of other major liquid simulated SBW constituents. Consequently, this feed simulated the SBW with overhead recycle flowsheet, in which most of the water and nitric acid from the SBW are evaporated, and the concentrated acid is neutralized and recycled back to the evaporator. This flowsheet would result in a single waste form as opposed to separate solid waste forms for evaporator overheads and bottoms.

1.3 Test Objectives

The primary objective of these tests was to demonstrate solidification of simulated liquid SBW with condensed, neutralized overhead recycle. Other objectives were as given below and parallel many of the objectives of past flask-scale and pilot-scale E/S tests, which were completed on simulated liquid SBW and simulated liquid SBW with tank heel solids. Due to the success of evaporating simulated SBW with heel solids in past ATFE tests, no solids were incorporated into these tests. This avoided the minor complications associated with a 2-phase feed (e.g., feed makeup and feeding to the evaporator) and analysis of bottoms samples that have insoluble solids.

1.3.1 Material and Energy Balance

This objective was to obtain data needed for calculation of complete material and energy balances for several overhead recycle conditions. Specifically, distillate composition, off-gas emission data, and data required to calculate overall heat transfer rates were desired.

1.3.2 Control of Evaporator Bottoms Concentration

This objective was to demonstrate that the bottoms concentration could be controlled by monitoring the bottoms temperature in a continuous process.

1.3.3 Fouling of Heating Surface

This objective was to record any evidence of fouling of the heating surface in the pilot-scale ATFE.

1.3.4 Plugging of Product Outlet

This objective was to document any problems with plugging the evaporator discharge during extended tests at steady-state conditions in the pilot-scale evaporator.

1.3.5 Waste Form Properties

This objective was to observe the time required to solidify and stabilize evaporator bottoms and to measure the physical properties of the evaporator bottoms.

1.3.6 Waste Form Critical Parameters Assessment

This objective was to evaluate the waste form for compliance against several disposal and transportation parameters, assuming the SBW liquid and heel solids are classifiable as TRU waste and eligible for WIPP disposal. The specific parameters evaluated in this report included the following: radiological properties, hydrogen generation and total gas limits, chemical compatibility, corrosivity/free liquids, and ignitability.

2. THEORY/EXPERIMENTAL APPROACH

The SBW precipitate that forms upon evaporation includes an aluminum nitrate salt that chemically binds up to nine water molecules for each aluminum nitrate molecule formed. The SBW can be concentrated by evaporation to the degree that the entire solution turns into a solid mass upon cooling. Aluminum sulfate is also present in the SBW and binds water molecules. Other SBW metals that form hydrates are calcium (Ca), iron (Fe), magnesium (Mg), manganese (Mn), and nickel (Ni). However, aluminum is 10 times more concentrated than the other elements. As the SBW concentrates in the presence of nitric acid, a solid binary compound with the SBW alkaline element nitrates occurs: $\text{KNO}_3 \cdot \text{HNO}_3$ and $\text{NaNO}_3 \cdot \text{HNO}_3$. These compounds could also aid in the formation of a solid bottoms product.

Flask-scale and pilot-scale tests were planned to evaluate E/S on SBW with overhead condensate neutralization and subsequent recycle back to the evaporator. The purpose for these tests was to investigate E/S flowsheets that minimize low-level waste volumes and off-gas emissions. Previous tests demonstrated that a minimum of 80% of the water and 80% of the nitric acid is evaporated from the SBW. Therefore, the flowsheet for SBW E/S treatment with overhead recycle assumes that the acid is separated from the water in the evaporator overheads either by a basic scrubbing process or by condensing and then concentrating the acid in an acid fractionator. If the acid fractionator were used, the concentrated acid would be neutralized, for example with magnesium oxide or aluminum hydroxide, and then mixed with the SBW feed to the evaporator. A block flow diagram for a SBW evaporation process with overhead recycle is presented in Figure 1.

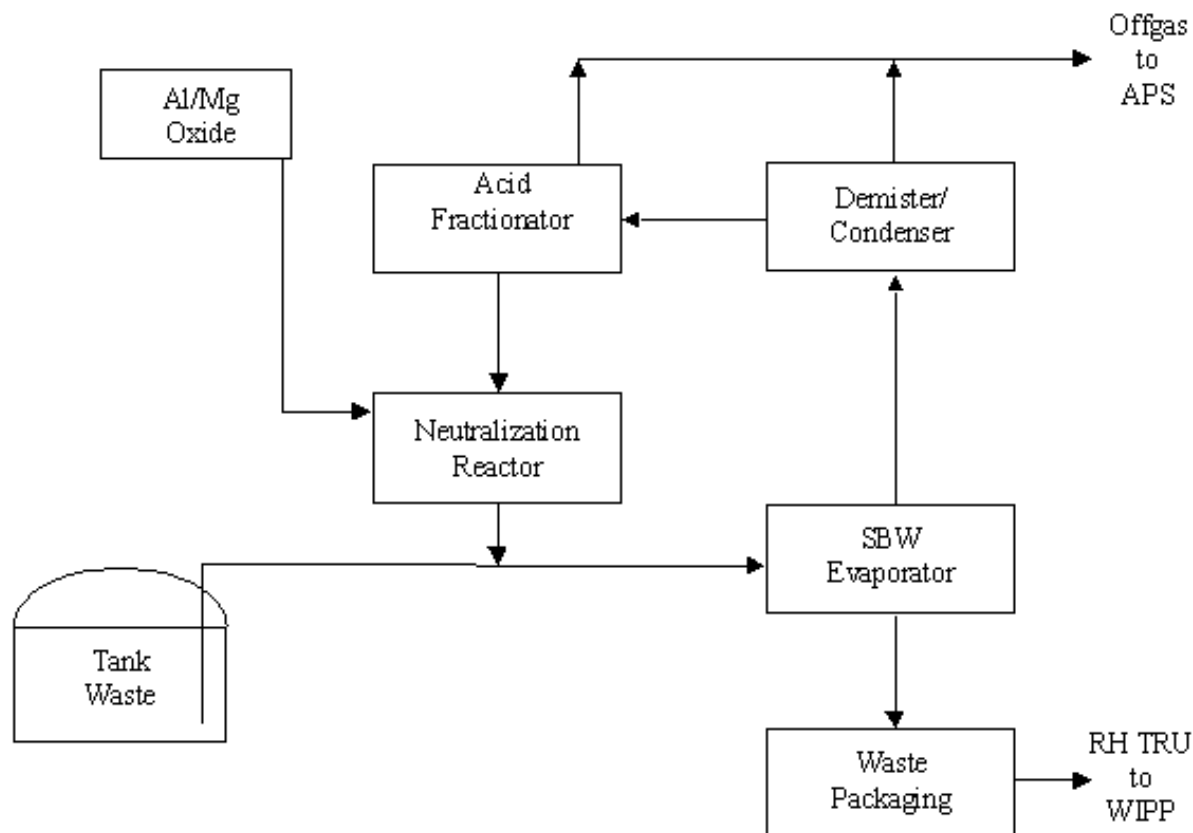


Figure 1. Direct evaporation with acid recycle block flow diagram.

Three recycle flowsheets were evaluated in the flask-scale test series to simulate overheads neutralization with (1) sodium hydroxide, (2) aluminum hydroxide, and (3) magnesium oxide. Two flask-scale tests were planned for each recycle condition to evaluate the bottoms and overhead characteristics at two different mass reduction ratios. Test conditions for the pilot-scale runs were identified from the results of the flask-scale tests.

Previous tests have demonstrated solidification of feeds that were high in aluminum nitrate. Consequently, a feed based on neutralizing the overhead acid with aluminum and recycling would be expected to produce bottoms material with desirable characteristics. However, no form of aluminum was identified that would readily dissolve in evaporator overhead solution. A high sodium feed based on neutralizing with caustic was tested at a flask-scale, but this feed was less likely to produce acceptable bottoms, because sodium nitrate does not form hydrates. Neutralizing with calcium oxide (lime) was considered, but calcium nitrate will not chemically bond with as much water as aluminum nitrate. It was concluded that magnesium nitrate would likely be an ideal choice. Magnesium oxide and magnesium hydroxide both dissolve rapidly and will neutralize evaporator overheads. Magnesium and aluminum both have the capability of chemically bonding with three moles of water per mole of nitric acid neutralized.

The approach for the flask- and pilot-scale tests was to increase the sodium, aluminum, or magnesium in the SBW surrogate to represent the proposed recycle composition. An SBW feed flowrate of 400 kg/hr was assumed for the composition calculations.⁷ Other key assumptions were that 85% of acid in the feed to the evaporator exits the evaporator with the overheads as nitric acid, and the acid fractionator bottoms is 50 wt% nitric acid and 50 wt% water. Feed composition calculations are summarized in Tables 1 and 2 for the magnesium recycle and aluminum recycle flowsheets, respectively. The WM-189 column is the base surrogate composition and the last column labeled “Feed” is the target composition for the tests.

Table 1. Target feed composition calculations for SBW with recycled magnesium-oxide-neutralized overheads.

	WM-189	Acid Fractionator Bot.	MgO	Recycle	Target Feed
Flow, kg/hr	400.00	92.15	14.74	106.88	506.88
Species	wt %	wt %	wt %	wt %	wt %
Al	1.44	— ^a	—	—	1.14
B	0.02	—	—	—	0.01
Ca	0.22	—	—	—	0.17
Cl	0.05	—	—	—	0.04
Cs	3.00×10^{-3}	—	—	—	2.00×10^{-3}
F	0.02	—	—	—	0.02
Fe	0.11	—	—	—	0.09
H	0.22	0.80	—	—	0.17
Hg	0.10	—	—	—	0.08
K	0.66	—	—	—	0.52
Mg	0.04	—	60.31	8.32	1.79

Table 1. (continued).

	WM-189	Acid Fractionator Bot.	MgO	Recycle	Target Feed
Mn	0.08	—	—	—	0.06
Na	3.53	—	—	—	2.78
NO ₃	34.22	49.20	—	42.42	35.95
SO ₄	0.77	—	—	—	0.61
Water	58.52	50.00	—	49.27	56.57

a. — = not applicable.

Table 2. Target feed composition calculations for SBW with recycled aluminum-hydroxide-neutralized overheads.

	WM-189	Acid Fractionator Bot.	Al(OH) ₃	Recycle	Target Feed
Flow, kg/hr	400.00	92.15	19.01	111.16	511.16
Species	wt %	wt %	wt %	wt %	wt %
Al	1.44	— ^a	34.59	5.92	2.42
B	0.02	—	—	—	0.01
Ca	0.22	—	—	—	0.17
Cl	0.05	—	—	—	0.04
Cs	3.00×10^{-3}	—	—	—	2.00×10^{-3}
F	0.02	—	—	—	0.02
Fe	0.11	—	—	—	0.09
H	0.22	0.80	—	—	0.17
Hg	0.10	—	—	—	0.08
K	0.66	—	—	—	0.52
Mg	0.04	—	—	—	0.03
Mn	0.08	—	—	—	0.06
Na	3.53	—	—	—	2.76
NO ₃	34.22	49.20	—	40.79	35.65
SO ₄	0.77	—	—	—	0.60
Water	58.52	50.00	—	53.30	57.38

a. — = not applicable.

The flask-scale and pilot-scale studies were run in the same test apparatuses as previous tests to evaluate the effects of overhead recycle on evaporator bottoms and off-gas characteristics. Specifically, the weight-percent of feed evaporated, the composition and handling characteristics of the bottoms, and the overhead composition were evaluated.

The experimental approach for each of the objectives listed in Section 1 is described below.

2.1 Material and Energy Balance

Material and energy balance data were collected in both flask and pilot-scale tests to gain a more complete understanding of the direct E/S process with overhead recycle. Surrogate feed was sampled after it was prepared for each test. A set of distillate and bottoms product samples was obtained for each test condition along with a complete set of readings, including feed rate, distillate rate, steam condensate rate, and system temperatures. Specific uses for the mass and energy balance information are discussed in the following sections.

2.1.1 Distillate Composition

Distillate consists primarily of water and nitric acid. The original baseline flowsheet for E/S includes neutralizing and grouting the distillate and disposing of it as low-level waste. The amount of grout varies directly with the amount of nitric acid in the overhead. However, the recycle flowsheet is based on neutralizing the acid that is boiled off and recycling it to the evaporator feed. Since the surrogate feed makeup for these tests includes an assumed recycle mass flow, it was important to compare the actual distillate flow with the amount assumed in the feed recipe.

Radionuclides are present in very low concentrations in SBW. An understanding of how these radionuclides partition in the E/S process is needed to complete the process design and plan for waste disposition. For example, the fission product cesium is known to be volatile at high temperatures, as in a vitrification process, but is not expected to be volatile at evaporator temperatures. However, because of its associated gamma activity, a fairly small amount of ^{137}Cs in the distillate could result in increased shielding requirements for the overhead process equipment. Various metals, representing radioactive elements, were added to the basic Tank WM-189 surrogate recipe and tested at the flask-scale to evaluate partitioning during E/S. Only non-radioactive cesium was added to the feed for the pilot-scale tests. Cesium was added at 10 times the actual concentration to ensure enough material in the feed and bottoms to produce accurate analytical results.

2.1.2 Off-Gas Emissions

The direct evaporation process includes a total condenser; therefore, off-gas emissions will only occur if non-condensable gas species are present. If there were no non-condensable species, it would be possible to operate the process with no vent to atmosphere. However, if a non-condensable stream were present, it would contain condensable components at their vapor pressure and also a small amount of mist.

The only non-condensable species that might be produced by the direct evaporation process are nitric oxide (NO) or nitrous oxide (N_2O), which result from the decomposition of nitrates. However, none of the nitrate salts present in SBW decompose at the evaporator operating temperature, so the amount of these produced will be small. This is one advantage of operating under vacuum.

Both the flask-scale and pilot-scale test systems are operated under a vacuum, so there is also a potential for air in-leakage. Additionally, the systems contain air at startup, and this air gets purged from the system by the first overhead vapor produced. Both systems utilize secondary condensers with chillers

to determine whether a significant amount of non-condensables are in the overheads. No secondary condensate was collected in previous tests, which indicated that very little non-condensable overheads were present to carry the condensable overheads beyond the primary condenser.

2.1.3 Overall Heat Transfer Rate

The material and energy balance data, along with the recorded operating steam temperatures, were used to calculate overall heat transfer coefficients for the pilot-scale tests.

2.2 Control of Evaporator Bottoms Concentration

The purpose of this objective is to determine if the evaporator's bottoms concentration can be controlled by the bottoms temperature during continuous operations in the ATFE tests. In the first pilot-scale test series, the evaporator steam temperature was adjusted so that the desired weight fraction of simulated SBW feed was boiled off. The feed boiloff was calculated by measuring the rate of overhead production at a constant controlled feed rate. In the second pilot-scale test series and in this third test series, the weight fraction boiled off was correlated with the evaporator bottoms temperature over a relatively wide range of conditions.

2.3 Fouling of Heating Surface

No evidence of fouling was indicated in previous pilot-scale tests. A higher potential exists for heating surface fouling in this pilot-scale test series for two reasons: (1) steady state conditions were maintained for longer periods and (2) fewer evaporator startup and shutdowns were planned, which means the evaporator gets rinsed with feed solution less frequently. The distillate-to-feed ratio will still be monitored as a potential indicator of fouling. A decrease in the ratio at constant waste feed and steam temperature would indicate the possibility of fouling, since the heat transfer will have changed due to salting, scaling, or fouling.

2.4 Plugging of Bottoms Outlet

The fraction of feed evaporated was increased to the point that plugging appeared to be imminent during the second pilot-scale test series. The third pilot-scale test series was operated at high bottoms concentrations for extended periods of time to verify that the bottom outlet does not plug during continuous operations.

2.5 Waste Form Properties

Solidification/stabilization times for the evaporator bottoms were recorded on the pilot-scale tests. The flask-scale tests were used to select the overhead recycle conditions that were tested in the pilot-scale unit. The operating conditions were selected based on the physical properties of the concentrated bottoms product obtained during the flask-scale tests. Observations on solidification times were recorded and drum headspaces were periodically checked for NO_x for the stored bottoms product from the pilot-scale tests. The pilot-scale product drums were measured for expansion of the external diameter of the drum to identify any gas pressurization or product expansion issues.

2.6 Waste Form Critical Parameters Assessment

The waste form was evaluated against several parameters derived from WIPP disposal and transportation requirements. The specific parameters are radiological properties, hydrogen generation and

total gas limits, chemical compatibility, corrosivity/free liquids, and ignitability. Due to time and experimental facility limitations, the waste form could not be evaluated against all of the WIPP requirements.⁸ Much of this evaluation was theoretical, but it gives some indication of the risk regarding whether a final E/S waste form can be shipped and disposed to the WIPP facility.

2.6.1 Radiological Properties

A detailed ASPEN model was previously generated to determine the fate of the radionuclides in the SBW feed in an evaporation process.⁹ The model accounted for overhead recycle. With overhead recycle, all radionuclides end up in the RH-TRU waste stream (evaporator bottoms), yielding a simple and reliable “Model.” A simple comparison of the volume reduction ratios between those calculated using the ASPEN model and those achieved during the pilot-scale test was used to ratio the radionuclide concentrations from the model to that expected from ATFE treatment with overhead recycle. This provides a very rough, theoretical estimate of the TRU alpha activity concentration. The radionuclide activity, fissile gram equivalents, ²³⁹Pu equivalent activity, radiation dose equivalent, and decay heat still need to be evaluated against the 72B shipping cask’s transportation and WIPP’s disposal requirements. Due to the lack of real waste (radioactive tests) data, the data generated from the model and cold experimental tests can only be used to make a statement regarding the risk that the waste form being produced (the solidified bottoms product) would not meet transportation and disposal criteria.

2.6.2 Hydrogen Generation and Total Gas Limits

The final waste forms water content was compared with the assumptions made in EDF-3392 to determine if the E/S waste form could exceed allowable hydrogen generation rates and total gas limits as identified in the 72B shipping cask’s Safety Analysis Report (SAR).¹⁰ A statement was made regarding the risk that the final waste form will not meet flammable gas and total gas limits for the 72B shipping cask.

2.6.3 Chemical Compatibility

Analysis of headspace gas samples from the sealed bottoms product containers were collected to determine if there is a risk that the final waste form produces a gas that is incompatible with the shipping container materials, other wastes, repository backfill, and repository seal and panel closure material. Previous flask- and pilot-scale tests demonstrated that the final waste form produces an off-gas as it cools and solidifies. The off-gas consists of water and NO_x [a combination of NO and nitrogen dioxide (NO₂)] and N₂O, which reacts to form nitric acid.

For the ATFE tests, plastic bags were taped over the tops of the evaporator bottoms drums to prevent vapor from escaping while the bottoms material cooled. Drager tubes were used to monitor NO_x levels in the headspace of the drums as they cooled. Once cooled, the lids were sealed to the drums. NO_x levels were measured when the drums were received at INTEC 29 days after the drums were sealed. The headspace of the drums was then purged with air and the drums re-sealed. Twenty-seven days later NO_x levels were measured in the drum headspace, the drum was purged with air, and the drum was re-sealed again. After this purge, the drums were monitored every few days to document the NO_x concentration changes in the headspace. The objective was to determine if cooled bottoms material continues to emit NO_x. The analysis provides an indication of the length of time a waste drum or canister must stabilize before it can be shipped in the 72B cask. Off-gassing could also impact the total gas limit in the 72B SAR as discussed in Section 2.6.2.

2.6.4 Corrosivity/Free Liquids

The final waste form was visually inspected to verify the absence of free liquids. Waste exhibiting the characteristic of corrosivity is prohibited at the WIPP facility. Corrosivity is a characteristic of liquids (aqueous with a $\text{pH} \leq 2$ or ≥ 12.5 or a liquid that corrodes steel at a rate > 6.35 mm/year at a temperature of 55°C); however, the presence of $<1\%$ residual liquids is allowed by WIPP. The SBW currently carries the U134 code, which means that the waste can contain “no residual liquids.” It is important to note that if the U134 code is removed then the liquid requirement would revert to $<1\%$ residual liquids.

2.6.5 Ignitability

A determination of whether the waste form is an oxidizer must be made. The waste form was visually inspected to determine whether it was monolithic, not friable, and not likely to be subject to decomposition during incidents normal to transport. If the waste form fails the visual exam (monolithic, non-friable, etc.), it would have to undergo future testing by the Department of Transportation (DOT) oxidizer Test Method 1040 to determine whether it is an oxidizer.

3. EXPERIMENTAL SETUP

Section 3 covers preparation of the evaporator feed, description of the experimental apparatus, and description of the test procedure.

3.1 Evaporator Feed Preparation

This series of tests was planned to evaluate E/S treatment of SBW with overhead recycle. The flowsheet for SBW with overhead recycle E/S treatment assumed that the acid is separated from the water in the evaporator overheads either by a basic scrubbing process or by condensing and then concentrating the acid in an acid fractionator. If an acid fractionator were used, the concentrated acid would be neutralized and then mixed, via a recycle loop, with the SBW being fed to the evaporator. The flask-scale test apparatus and the ATFE pilot plant do not have capability to continuously recycle condensate from the primary condenser back to the evaporator, so the surrogate feed recipe for these tests was modified to include the recycle materials.

The feed for these tests was a surrogate based on analysis of samples taken from Tank WM-189.¹¹ The composition was adjusted for overhead neutralization and recycle as described in Section 2. In general, only the major components were added to the surrogate. However, several metals were added to the flask-scale tests, and non-radioactive cesium was added to the pilot-scale tests to determine their partition factors. The target feeds for each recycle flowsheet are given in Table 3. Chromium, copper, fluorine, lead, nickel, and phosphorus were added to the surrogate for the flask-scale tests at a total concentration of 0.064 wt%. Chlorine was not added to the pilot-scale surrogate feed. The following sections discuss feed preparation and final composition in detail as determined from chemical analysis.

Table 3. Target feed compositions for flask- and pilot-scale tests.

Component	Sodium Recycle, wt%	Magnesium Recycle, wt%	Aluminum Recycle, wt%
H ₂ O	54.96	56.57	57.38
Acid	0.17	0.17	0.17
Aluminum	1.11	1.14	2.42
Boron	0.01	0.01	0.01
Calcium	0.17	0.17	0.17
Chlorine	0.05	0.04	0.04
Cesium	2×10^{-3}	2×10^{-3}	2×10^{-3}
Fluorine	0.02	0.02	0.02
Iron	0.08	0.09	0.09
Mercury	0.08	0.08	0.08
Magnesium	0.03	1.79	0.03
Manganese	0.06	0.06	0.06
Potassium	0.51	0.52	0.52
Sodium	6.04	2.78	2.76
Nitrate	36.04	35.95	35.65
Sulfate	0.61	0.61	0.60
Total	99.94	100.00	100.00

3.1.1 Flask-Scale Tests

Three recycle flowsheets were tested: overheads neutralized with (1) magnesium oxide, (2) aluminum hydroxide, and (3) sodium hydroxide. One- to two-L batches were prepared of each feed type, following the recipes given in Section 3.1 and using the makeup procedure outlined in Section 4.3.¹² The tests were labeled FSR-XX-Y, where FSR is flask-scale recycle, XX is the neutralizing additive, and Y is the test number. Samples were submitted to the INTEC Analytical Laboratory to confirm the feed composition for each. The chromatographic method used for the nitrate analysis was inaccurate due to the formation of complex molecules with aluminum and iron that form in the SBW surrogate. To correct for this inaccuracy, the stoichiometric concentration of nitrates was calculated based on the cation concentrations. Analyses were not requested on several of the minor constituents: chromium, copper, fluorine, lead, nickel, and phosphorus although they were added to the feed. The feed compositions used in the mass balances are summarized in Table 4.

Table 4. Actual flask-scale feed compositions.

Component	FSR-1 (Na) and FSR-2 (Na), wt%	FSR-5 (Mg) and FSR-6 (Mg), wt%	FSR-3 (Al) and FSR-4 (Al), wt %
H ₂ O	56.62	62.54	55.53
Acid	0.16	0.14	0.17
Aluminum	1.00	1.05	2.45
Boron	0.01	0.01	0.01
Calcium	0.15	0.16	0.17
Chlorine	0.07	0.03 ^a	0.03
Chromium	0.01	0.01	0.01
Cesium	3×10^{-3}	3×10^{-3}	3×10^{-3}
Copper	NA ^b	NA ^b	NA ^b
Fluorine	NA ^b	NA ^b	NA ^b
Iron	0.08	0.09	0.09
Lead	NA ^b	NA ^b	NA ^b
Magnesium	0.03	1.18	0.03
Manganese	0.06	0.06	0.07
Nickel	NA ^b	NA ^b	NA ^b
Phosphorus	NA ^b	NA ^b	NA ^b
Potassium	0.54	0.49	0.53
Sodium	6.04	2.71	3.00
Nitrate	25.65	18.54	28.73
Nitrate calculated	34.86	31.13	37.50

Table 4. (continued).

Component	FSR-1 (Na) and FSR-2 (Na), wt%	FSR-5 (Mg) and FSR-6 (Mg), wt%	FSR-3 (Al) and FSR-4 (Al), wt %
Sulfate	0.28	0.33	0.31
Mercury	0.08	0.07	0.08
Total ^c	90.78	87.41	91.21
Total ^c	99.99	100.00	99.98

a. Calculated value.

b. NA – not analyzed.

c. Using the analytical nitrate concentration.

d. Using the calculated nitrate concentration.

3.1.2 Pilot-Scale Tests

Two recycle flowsheets were tested: overheads condensed and neutralized with magnesium oxide and overheads condensed and neutralized with aluminum hydroxide. Below is the feed preparation description for each flowsheet.

Three hundred seventy-eight liters (100 gal) of Tank WM-189 surrogate with magnesium recycle were prepared in a 946-L (250-gal) tank with an anchor-type agitator. The feed was then transferred to 208-L (55-gal) drums and duplicate 100-mL samples collected. The tests were labeled MG-X, where MG stands for SBW with magnesium-oxide-neutralized overheads and X is the run number.

Four hundred seventy-three liters (125-gal) of WM-189 surrogate with aluminum recycle were prepared in a 946-L tank with an anchor-type agitator. The feed was then transferred to 208-L (55-gal) drums and duplicate 100-mL samples collected. The tests were labeled AL-X, where AL stands for SBW with aluminum-hydroxide-neutralized overheads and X is the run number.

The samples were submitted to the INTEC Analytical Laboratory to confirm the feed composition for each feed. The chromatographic method used for the nitrate analysis was inaccurate due to the formation of complex molecules with aluminum and iron that form in the SBW surrogate. To correct for this inaccuracy, the stoichiometric concentration of nitrates was calculated based on the cation concentrations. Analyses were not completed on the fluoride. The feed compositions that were used in the mass balance analysis are summarized in Table 5.

3.2 Experimental Apparatus

3.2.1 Flask-Scale Tests

Flask-scale tests were batch tests run with approximately 750 mL of the SBW with overheads recycle surrogate. A schematic of the flask-scale test apparatus is shown in Figure 2. The experimental apparatus consisted of a glass flask containing the feed surrogate fitted with a condenser and a heating mantle. The general procedure for all tests was to boil the surrogate in the flask. The bottoms were poured from the flask into a poly bottle for the FSR Runs 1, 3, 5, and 6. For Runs 2 and 4, the bottoms remained in the boiling flask. Runs 2 and 4 were “cooked” to a solid mass. The condensate was collected in a subcooled flask (cooled to <8°C).

Table 5. Actual pilot-scale feed compositions.

Component	Magnesium Recycle (MG-1, MG-2), wt%	Aluminum Recycle (AL-1, AL-2), wt%
Water	59.48	58.81
Acid	0.15	0.15
Aluminum	1.07	2.60
Calcium	0.16	0.16
Cesium	0.02	0.02
Fluorine	NA ^a	NA ^a
Iron	0.09	0.08
Magnesium	1.72	0.03
Manganese	0.06	0.06
Potassium	0.55	0.45
Sodium	2.82	2.61
Nitrate	33.68 ^b	34.84 ^b
Sulfur	0.22	0.21
Total	100.00	100.00

a. NA – not analyzed.

b. Calculated nitrate concentration.

Thermocouples were used to monitor the following temperatures: boiling flask solution (to 140°C), boiling flask vapor (to 130°C), upper heating mantle (to 130°C), lower heating mantle (to 300°C), subcooled condensate (-10 to 15°C), and the off-gas at its volume measurement points. A condenser was attached to the flask to enable vapor condensate recovery with the cooling solution near 0°C. A vacuum pump was used to evacuate the system and to lower the absolute pressure to about 260 mm Hg absolute, enabling the solution to boil at lower temperatures. System absolute pressure at the flask was monitored and the pump rate adjusted as needed.

System instruments were checked against calibrated instrumentation and were within $\pm 2\%$ accuracy.

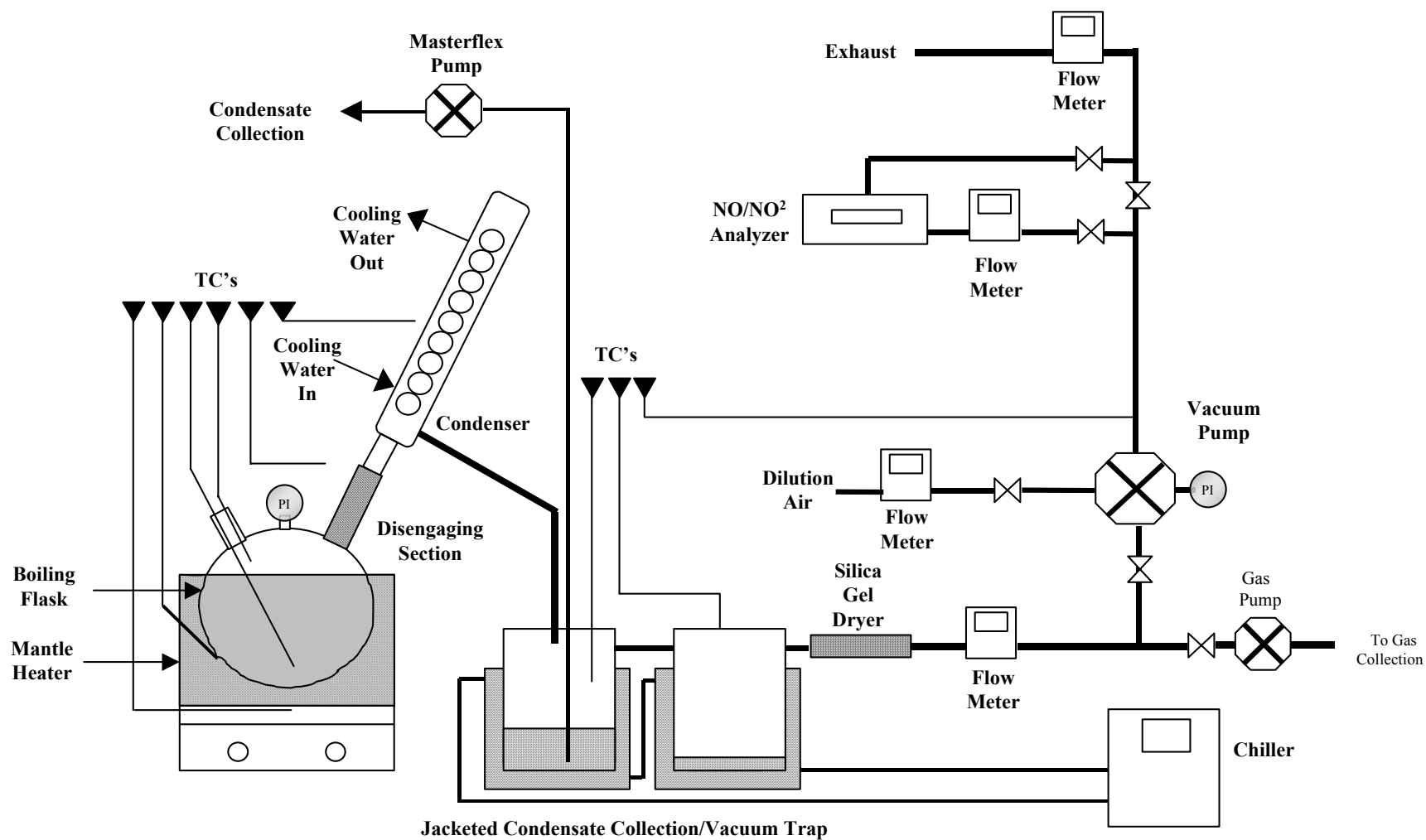


Figure 2. Flask-scale test apparatus.

3.2.2 Pilot-Scale Tests

Pilot-scale tests were carried out in an ATFE at LCI Corporation's Charlotte, NC, facility. Each test used between 379–568 L of SBW surrogate feed. The same experimental setup was used for this series of pilot-scale tests as was used for the previous series. A flow diagram is given in Figure 3. A peristaltic pump was used to move feed through a mass flow meter, backpressure valve, and preheater to the top of the evaporator. A rigid three-blade rotor covered the length of the heated section, provided agitation, and produced a uniform thin film on the evaporator heat transfer surface. A photograph of the rotor can be seen in Figure 4. The clearance between the rotor and the evaporator wall was 0.76 mm (0.030 in.). The rotor was operated at 1,800 rpm, resulting in a tip speed of 8 m/s. The rotor was gear-driven, powered by an electric motor, and had a bottom bearing that rode on a cone at the bottom of the heated section. Figure 5 is a photograph of the inside of the evaporator and it shows the cone that centers the bottom bearing. Three spokes centered the cone, and the top of the rotor had a baffle to disengage mist.

The ATFE had a heating surface area of 0.13 m² (1.4 ft²) and an inside diameter of 7.62 cm. It was heated with steam and the steam pressure was controlled manually with a regulator to achieve the desired evaporation rate. The bottom of the evaporator consisted of a cone with a 5-cm outlet immediately below the cylindrical heated section. During operation, bottoms drained continuously from the bottom of the evaporator into a timed discharge system.

At the inlet to the timed discharge system, the bottoms material passed through a view port and then through a small accumulator (not shown in Figure 3) followed by a 5-cm (2-in.) ball valve that was normally open. The bottoms material then dropped into the 20-L timed discharge vessel. A second 5-cm (2-in.) ball valve that was normally closed was at the bottom outlet of the timed discharge vessel. The timed discharge sequence was automatically initiated once every 6 minutes. This time interval was chosen to make it convenient to convert the mass accumulated in the bucket to kg/hr by moving the decimal point (since 6 minutes is 1/10 of an hour). The discharged material was collected in stainless steel buckets and transferred to 15-gal drums. The discharge sequence was as follows:

1. The inlet valve to the timed discharge vessel closed.
2. The timed discharge vessel was pressurized with nitrogen.
3. The outlet valve opened for a few seconds discharging accumulated bottoms material.
4. The outlet valve closed.
5. The timed discharge vessel was evacuated to approximately the same pressure as the evaporator.
6. The inlet valve opened.

The planned feed rate was about 11.6 mL/s, corresponding to a planned bottoms rate of about 3.3 mL/s. Based on an average volumetric flow rate of 7.5 mL/s, the residence time of material in the heating zone was only 13 seconds. Since no back-mixing occurs in the evaporator, process steady state is reached in one residence time after an input change is made, assuming the temperature remains constant. However, previous tests demonstrated that even though the process reached steady state quickly, the bottoms discharge rate could not be measured accurately due to the viscous bottoms material hanging up in the timed discharge system. Consequently, the bottoms discharge rate was determined by the difference between the feed and distillate rates. The run times for these tests were extended to ensure that the timed discharge system holdup would not impact data analysis.

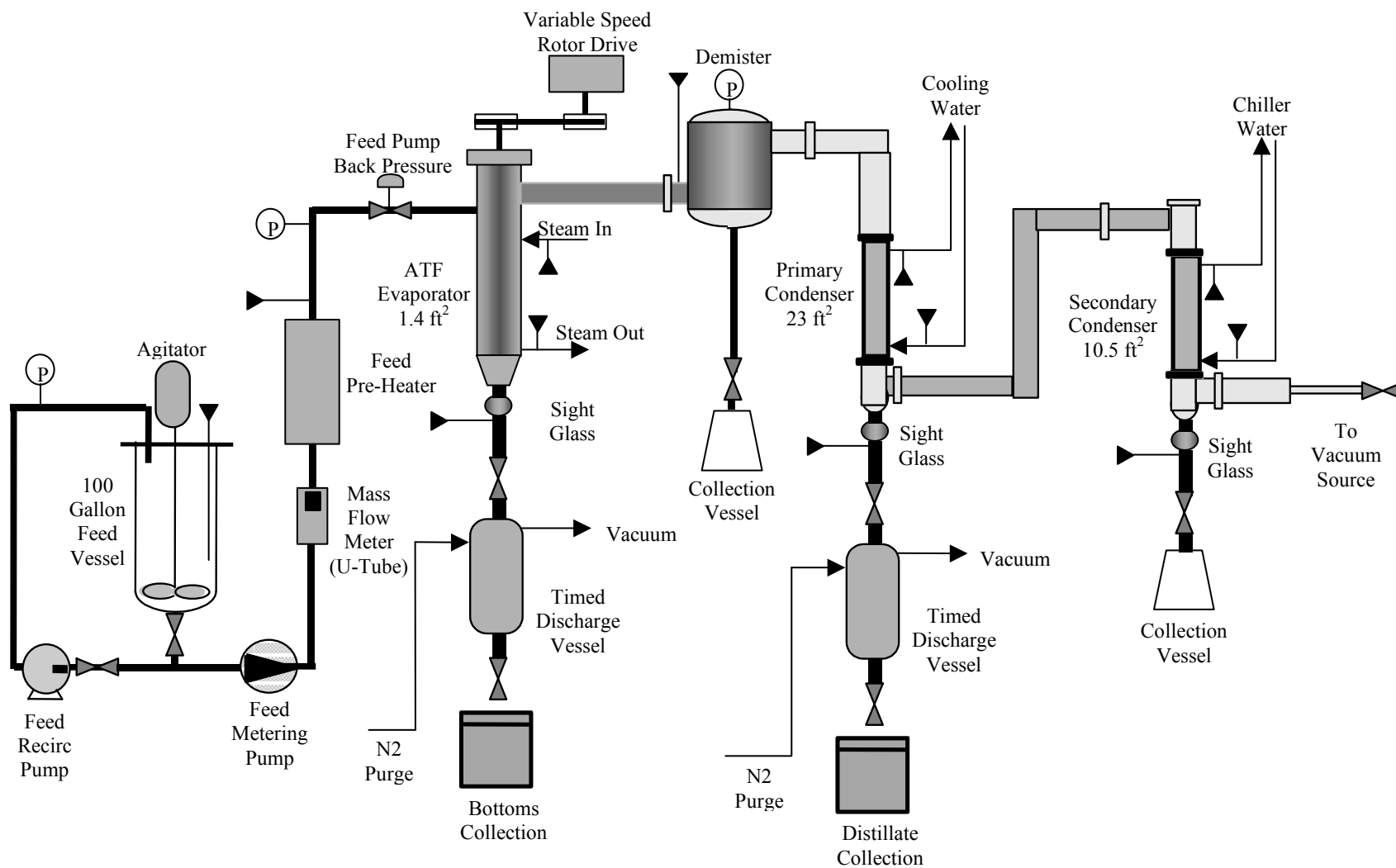


Figure 3. Agitated thin film evaporator pilot plant.



Figure 4. Evaporator rotor.



Figure 5. Normal appearance inside the evaporator.

The distillate outlet nozzle was on the side of the evaporator immediately above the rotor and heated section. The distillate passed through a wire mesh mist eliminator (demister), a water-cooled primary condenser, and then a secondary condenser that used chilled coolant. Vacuum was provided by a liquid ring vacuum pump. A control valve that bled ambient air in at the vacuum pump inlet automatically controlled evaporator vacuum. This was the only feedback control loop in the system. Vacuum was maintained at approximately 380 mm Hg.

Condensate from the primary condenser was discharged by a timed discharge system that was similar to the bottoms discharge system. The condensate collection bucket was then emptied into 208-L drums. Condensate from the secondary condenser and liquid from the demister were collected in 4-L flasks.

Adjusting the speed of the peristaltic feed pump controlled the feed rate. The feed rate was checked for each feed by measuring the mass of feed collected in a bucket in 6 minutes.

A data acquisition system recorded electronic data once per minute, including system pressure, steam temperature, bottoms temperature, distillate temperature, feed rate, and feed temperature.

Figure 6 is a photo of the ATFE pilot plant with the evaporator in the center. The drive motor, transmission, belt, rotor pulley, and evaporator top flange are all visible at the top. Upon close examination, the evaporator bottom outlet view port can be seen near the center of the figure. The timed discharge system is below the view port and the demister drain line is immediately to the left of the evaporator with a 4-L flask attached. The timed discharge system for the condensate is to the left of the demister drain line. The condenser discharge system is uninsulated but is similar to the evaporator discharge system. Figure 7 is a close-up of the condensate discharge system. The evaporator discharge system includes a small accumulator between the view port and the inlet valve to the timed discharge vessel. The condensate discharge system does not include a similar accumulator. Presumably, it was acceptable for a small amount of distillate to accumulate in the bottom of the condenser when the inlet to the timed discharge vessel was closed.



Figure 6. Agitated thin film evaporator.



Figure 7. Condensate discharge system.

3.3 Test Procedure

3.3.1 Flask-Scale Tests

Three SBW with overhead recycle surrogate feed compositions were tested: (1) sodium-hydroxide-neutralized overheads, (2) aluminum-hydroxide-neutralized overheads, and (3) magnesium-oxide-neutralized overheads. Two tests were run with each feed composition: one at a mass reduction ratio of 60 wt% and another concentrated as much as practical. Table 6 lists the feed and conditions tested.

Table 6. Flask-scale test conditions.

Test #	Feed Composition	Target Mass Reduction
FSR-1 (Na)	WM-189 surrogate w/sodium-hydroxide-neutralized overhead recycle	~60 wt%
FSR-2 (Na)	WM-189 surrogate w/sodium-hydroxide-neutralized overhead recycle	Maximum achievable
FSR-3 (Al)	WM-189 surrogate w/aluminum-hydroxide-neutralized overhead recycle	~60 wt%
FSR-4 (Al)	WM-189 surrogate w/aluminum-hydroxide-neutralized overhead recycle	Maximum achievable
FSR-5 (Mg)	WM-189 surrogate w/magnesium-oxide-neutralized overhead recycle	~60 wt%
FSR-6 (Mg)	WM-189 surrogate w/magnesium-oxide-neutralized overhead recycle	Maximum achievable

Flask-scale tests were performed to determine an appropriate mass reduction ratio for each recycle flowsheet. The bottoms product characteristics such as pourability, solidification capability, and product toughness (e.g. hardness, non-friable/monolithic) were evaluated for acceptability. The feed carryover to the overheads, particularly acid, was evaluated against the product characteristics. For each test run, a charge of approximately 750-mL of the waste (SBW and neutralized overheads) surrogate was added to the pre-weighed 1.0-L flask. The flask was attached to the apparatus and the heat mechanism started. Temperature was continuously monitored via thermocouples and a remote data logger, and other data were taken manually. Vapors leaving the heated flask condensed at temperatures from 3 to 10°C, which is below the normal boiling point of NO₂. Most of the NO₂ reacts with the water to produce NO, plus nitrous and nitric acid. Vapors passing through the condenser and the condensate entered the subcooled collection vessel at a temperature between 0 and 3°C. Next, the vapor entered the vacuum trap followed by the silica gel drier where any remaining water was collected.

Thermocouples were used to monitor the solution temperature, outside flask temperature (mantle temperature), vapor above the solution, subcooled condensate, and off-gas at the volume measurement points. A condenser was attached to the flask to enable vapor condensate recovery with the cooling solution near 0°C. A vacuum pump was used to lower the absolute pressure, enabling the solution to boil at lower temperatures. System absolute pressure at the flask and vacuum pump were monitored.

The SBW surrogate was concentrated by evaporation to the predetermined end points (see Table 6) based on the volume of overheads condensate collected. The concentrated solution was poured from the flask and allowed to naturally cool to ambient temperature for all but Runs 2 and 4, allowing solidification to occur. Runs 2 and 4 were concentrated to the extent that it could not be poured from the flask. After the solidification step, any sign of remaining liquid was noted.

3.3.2 Pilot-Scale Tests

The results from the flask-scale tests were used to identify the feed compositions and operating parameters for the pilot-scale tests. Two feed compositions were tested: the first simulating a magnesium-neutralized overheads recycle and the second simulating an aluminum-neutralized overheads recycle. For each feed composition, two mass reduction target values were identified: 55% and 65% (or achievable high limit). The test number and experimental parameters are summarized in Table 7.

Surrogate SBW with overhead recycle feed was added to the feed tank, mixed for about 30 minutes, and a feed sample taken from the feed pump discharge. The feed rate was set by adjusting the speed of the peristaltic feed pump and measured by weighing the amount of feed collected in a bucket over a 6-minute period. The feed throughout the runs was constant at approximately 54.4 kg/hr (120 lb/hr).

After feed was started to the evaporator, the steam temperature was gradually increased using a pressure regulator until the target mass reduction ratio was achieved, based on the feed and distillate rates.

Table 7. Test parameters for LCI Series 3 tests.

Test #	Feed Composition	Target Mass Reduction
AL-1	WM-189 with aluminum recycle	55%
AL-2	WM-189 with aluminum recycle	65%
MG-1	WM-189 with magnesium recycle	55%
MG-2	WM-189 with magnesium recycle	65%

Once the mass reduction ratio was reached, the system was operated at steady state until a 15-gal drum of bottoms was produced or the feed tank was empty. Bottoms and overhead samples were collected at two different times during each run. The first set was collected after about 2 hours of steady-state operation and the second near the end of the run. Data collected at the time of sampling included feed, bottoms, and distillate rates, temperatures (feed, bottoms, vapor separator, vapor, steam heat in, steam heat out, condenser in, condenser out, and distillate) and pressure. Other data collected included the ATFE rotor speed, power, distillate ratio, feed pump setting, and feed tank temperature.

4. TEST RESULTS

Section 4 gives detailed information on the material and energy balance, discusses the control of the concentration of the evaporator bottoms, describes fouling of the heating surface, describes plugging of bottoms discharge, gives details on waste form properties, and assesses waste form critical parameters.

4.1 Material and Energy Balance

Material and energy balance covers composition of the distillate, off-gas emissions, and the overall heat transfer rate.

4.1.1 Distillate Composition

4.1.1.1 Flask-Scale Tests. With the exception of mercury, chloride, acid, water, and boron, the total carryover/evaporation of feed materials to the distillate was less than 0.001 wt%. The mass fraction of acid in the feed that was identified in the overheads against the equivalent percent of the feed mass evaporated is plotted in Figure 8. The sodium recycle flowsheet had higher concentrations of acid evaporated to the overheads than did the magnesium and aluminum recycle flowsheets. The aluminum recycle flowsheet had the least acid evaporated to the overheads at a given equivalent percent feed concentration.

Figures 9, 10, and 11 are plots of the mercury and chloride concentrations (as a wt% of feed) accumulated in the overheads against the total equivalent feed evaporated. At the desired operational equivalent concentration, the sodium recycle flowsheet had the least mercury and chlorine partition to the overheads at approximately 2–11 wt% and 11–14 wt% of the feed concentrations, respectively (Figure 9), but the sodium flowsheet was not operable. No pourable product could be formed because

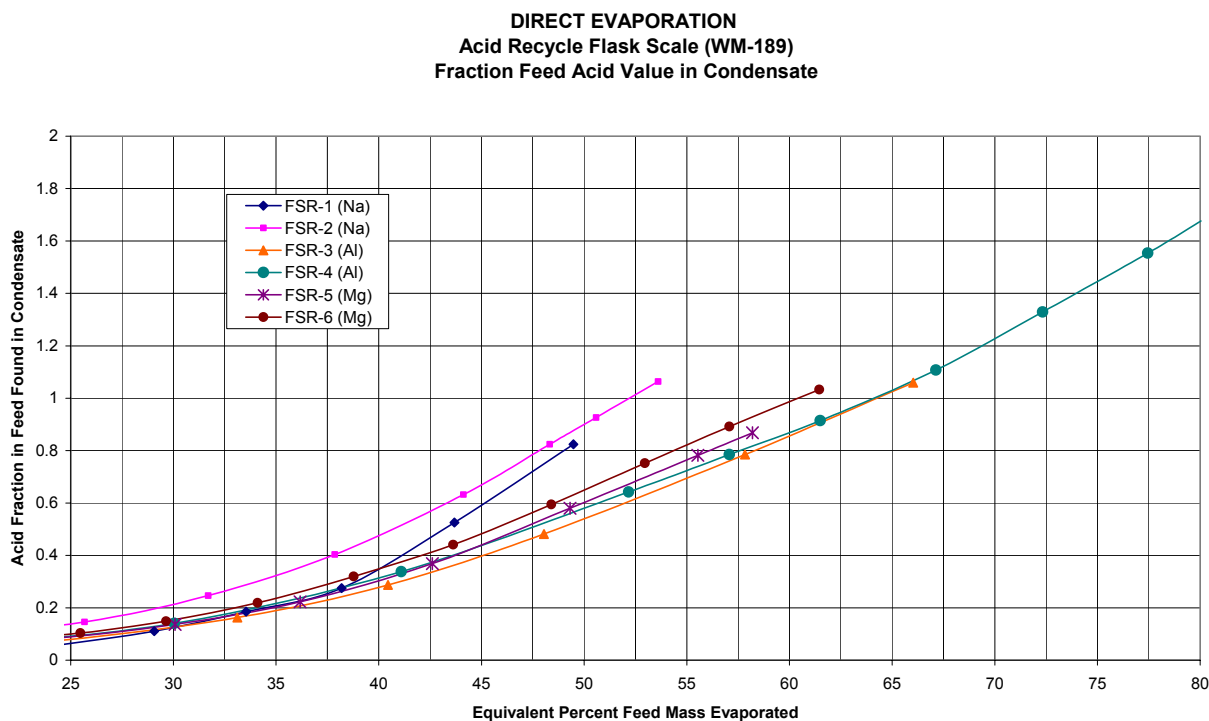


Figure 8. Acid feed fraction in distillate.

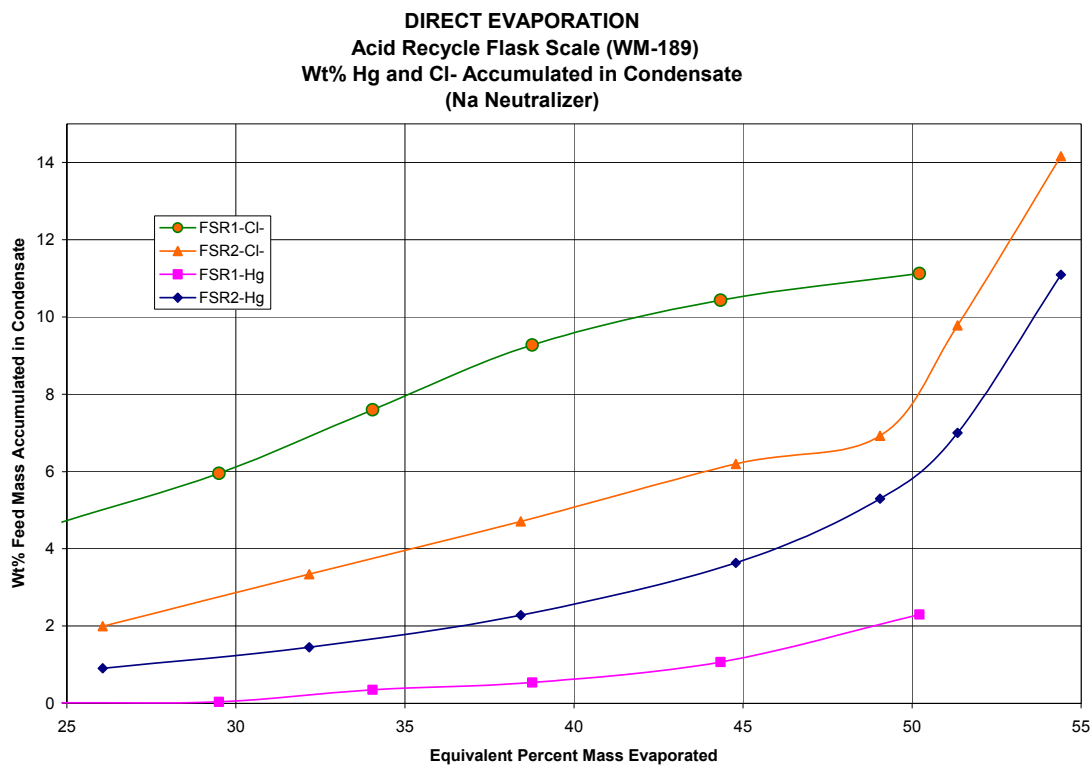


Figure 9. Weight% mercury and chloride accumulated in the overheads for the sodium-neutralized recycle flowsheet.

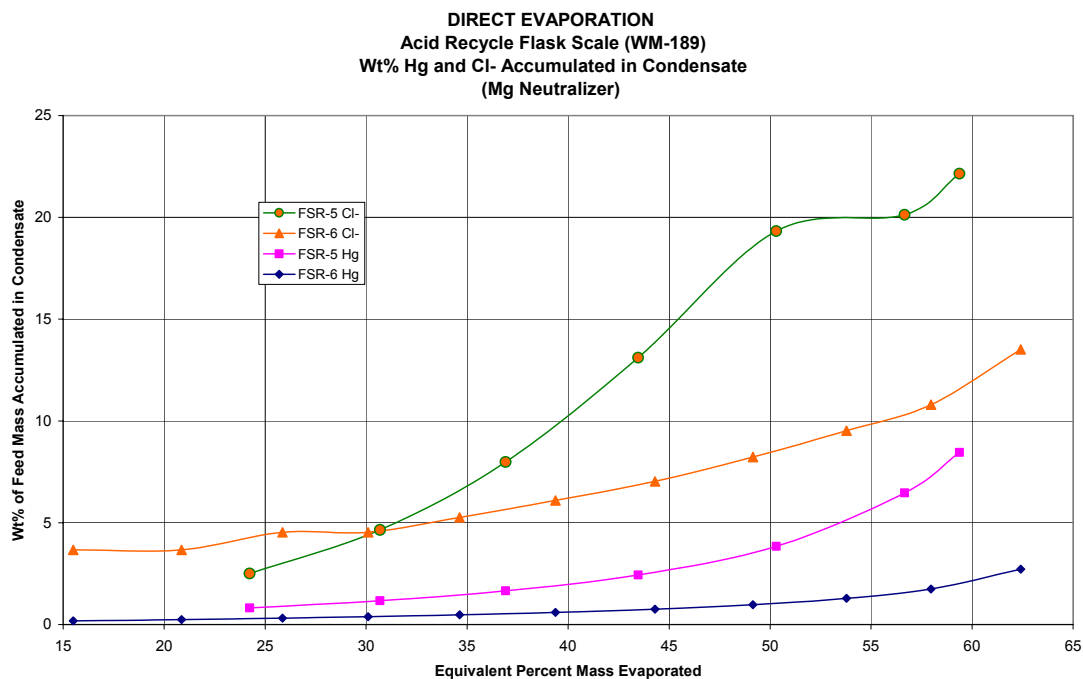


Figure 10. Weight% mercury and chloride accumulated in the overheads for the magnesium-neutralized recycle flowsheet.

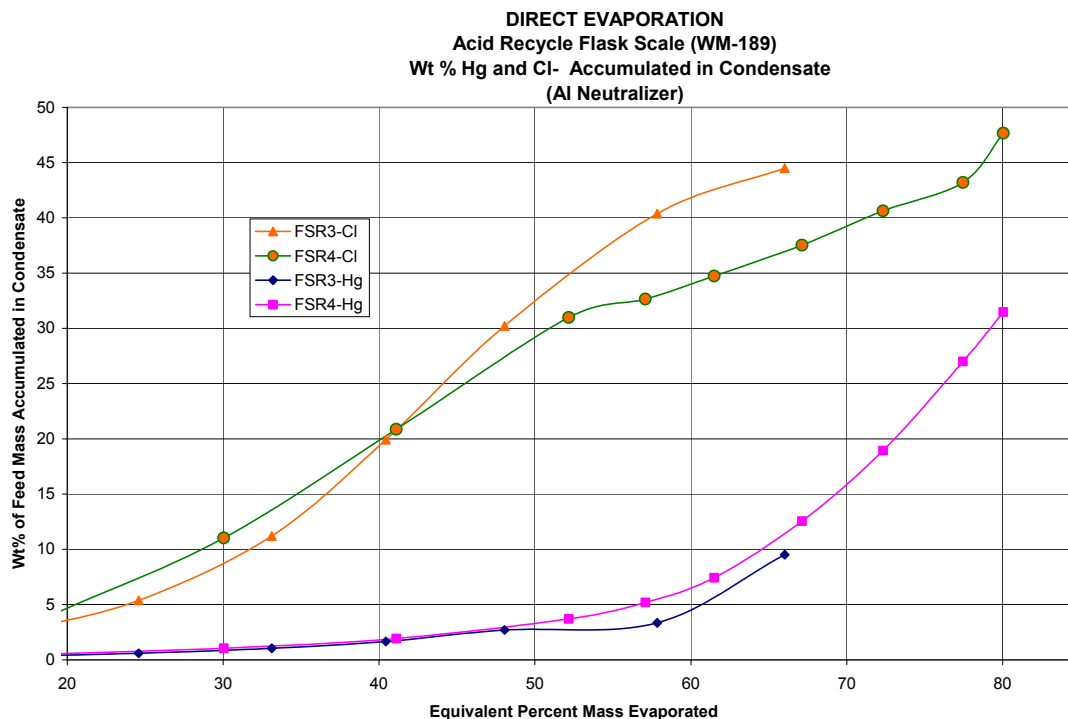


Figure 11. Weight% mercury and chloride accumulated in the overheads for the aluminum-neutralized recycle flowsheet.

of the excessive formation of sodium nitrate crystals in the bottoms. For the desired operational range with the magnesium flowsheet, mercury and chloride partitioned to the overheads at approximately 2–8 wt% and 10–23 wt% of the feed concentrations, respectively, for the magnesium recycle flowsheet. The aluminum recycle flowsheet had overhead mercury and chlorine concentrations at 4–6 wt% and 30–42 wt% of the feed concentrations, respectively.

In summary, none of the Hg concentrations exceeded 10 wt% of the feed unless pushed to a high and unreasonable equivalent concentration. For most practical purposes, the recycle flowsheet needs to be restricted to below 60 wt% equivalent mass evaporated to inhibit the formation of extra acid as is shown in Figure 8. Only the aluminum runs produced a concentration of chloride in the overheads greater than 20 wt% of feed. The aluminum recycle flowsheet demonstrated very high mercury and chloride volatilization rates.

4.1.1.2 Pilot-Scale Tests. The distillate was sampled and analyzed to determine its composition. Table 8 summarizes the amount, in wt%, of feed that partitioned to the overheads and was found in the distillate of the primary condenser.

The acid in the distillate was higher than predicted by the flask-scale tests. In all cases, the amount of acid in the overheads exceeded the amount of acid in the feed. This indicates that nitrates were being converted to oxides or hydroxides in the evaporator.

As in previous tests, very little of the non-volatile species was found in the distillate. The exception was iron, which suggests corrosion in the condenser or piping.

Table 8. Weight percent of each feed component that partitioned to the distillate.

	AL-1-1	AL-1-2	AL-2-1	AL-2-2	MG-1-1	MG-1-2	MG-2-1	MG-2-2
Feed rate, kg/hr	58	58	54.9	54.9	60.3	60.3	54.9	54.9
Run time, hr	2	4.3	2	5.75	2.75	5.5	2.25	5
Wt% feed evaporated	53.9%	53.9%	62.0%	62.8%	57.9%	54.1%	61.2%	63.6%
	Wt%	Wt%	Wt%	Wt%	Wt%	Wt%	Wt%	Wt%
Acid	106.85	109.97	151.94	156.13	128.90	110.71	142.54	151.78
Cesium	<0.008	<0.008	<0.015	<0.015	<0.013	<0.013	<0.014	<0.015
Aluminum	0.004	0.003	0.003	0.005	0.023	0.006	0.008	0.007
Calcium	0.053	0.014	0.009	0.013	0.058	0.015	0.018	0.017
Iron	0.266	0.217	0.336	0.454	1.148	0.286	0.256	0.349
Magnesium	0.223	0.090	0.104	0.139	0.014	0.007	0.008	0.009
Manganese	0.010	0.008	0.009	0.014	0.031	0.014	0.012	0.016
Potassium	0.003	0.003	0.004	0.004	0.020	0.005	0.008	0.006
Sodium	0.003	0.003	0.003	0.004	0.016	0.005	0.007	0.006
Sulfate	0.009	0.007	0.006	0.006	0.021	0.006	0.008	0.008
Nitrate	27.38	28.18	38.93	40.01	34.51	29.63	38.15	40.62
Water	75.18	74.70	81.96	82.72	77.47	73.96	80.87	83.61
Bottoms rate, kg/hr	26.8	26.8	20.9	20.4	25.4	27.7	21.3	20.0

Cesium was of particular interest, because ^{137}Cs is responsible for most of the gamma radiation in SBW. The presence of cesium in the distillate could complicate processing of the overheads in an acid fractionator by requiring that the process be shielded. However, results indicate that cesium is non-volatile under these conditions, even though it was present in the feed at 10 times the concentration in actual SBW.

4.1.2 Off-Gas Emissions

Table 9 shows primary and secondary condenser temperatures recorded during each ATFE run. The distillate consists of 20 wt% nitric acid. The vapor pressure corresponding to each temperature is also shown in Table 9. The mole % of condensable material that would be present in an off-gas stream is also presented based on the system operating pressure of 380 mm Hg absolute. At this pressure, the boiling point of 20 wt% nitric acid is 85 °C. Thus, a primary condenser temperature of less than 85 °C would result in no off-gas emissions if there were no non-condensable species.

In all but one case there was no observable secondary condensate, indicating that there was negligible non-condensable off-gas. The one exception was during Run AL-1-1 when the primary condenser was unintentionally operated at 66.5 °C. It was estimated that 5–10 g of condensate were collected from the secondary condenser at that time. It would take less than one standard cubic foot (scf) of non-condensable gas to carry that much condensable vapor to the secondary condenser based on the vapor pressures recorded in Table 9. However, if one scf of non-condensable vapor was produced per run, an additional 8.5 mL should have been collected in the secondary condensate flask during the remainder of the test series. Instead, the secondary condensate flask was emptied after Run AL-1-2, and no more secondary condensate was collected.

Table 9. Primary and secondary condenser temperatures.

Run	Primary Condenser			Secondary Condenser		
	Outlet Temp., °C	Vapor Pressure, mm Hg	Mole % Volatiles, y_i	Outlet Temp., °C	Vapor Pressure, mm Hg	Mole % Volatiles, y_o
AL-1	66.5	173.6	45.7	15.9	11.7	3.1
AL-2	26.7	23	6.1	16.7	12.4	3.3
AL-3	30.3	28.1	7.4	14.5	10.6	2.8
AL-4	31.5	30.3	8.0	14.9	10.8	2.8
MG-1	35.2	36.9	9.7	16.1	11.8	3.1
MG-2	34.4	35.4	9.3	16.7	12.4	3.3
MG-3	33.0	32.9	8.7	15.2	11.1	2.9
MG-4	33.4	33.6	8.8	17.0	12.6	3.3

4.1.3 Overall Heat Transfer Rate

As in the first and second series of pilot-scale tests in the ATFE at LCI, an overall heat transfer coefficient for the evaporator was calculated for each run. This overall heat transfer coefficient is defined by the following equation:

$$Q = U A \Delta T_{\text{Log Mean}}$$

Where

Q = evaporator heat duty (W)

U = overall heat transfer coefficient ($\text{W}/\text{m}^2/^\circ\text{C}$ or $^\circ\text{K}$)

A = surface area of the evaporator (m^2)

$\Delta T_{\text{Log Mean}}$ = log mean temperature difference ($^\circ\text{C}$) = $(\Delta T_1 - \Delta T_2)/\ln(\Delta T_1/\Delta T_2)$.

The evaporator heat duty was calculated from the material balance and temperatures recorded for each run. For the purpose of the material balance, the bottoms composition and flow were calculated by subtracting the distillate from the feed. This is the most accurate way to determine the bottoms composition leaving the evaporator. The log-mean temperature difference was calculated from the feed temperature, outlet steam temperature, and bottoms temperature. This is based on the assumption that the steam is saturated and has a constant temperature within the evaporator. The values used to calculate the log-mean temperature difference are shown conceptually in Figure 12.

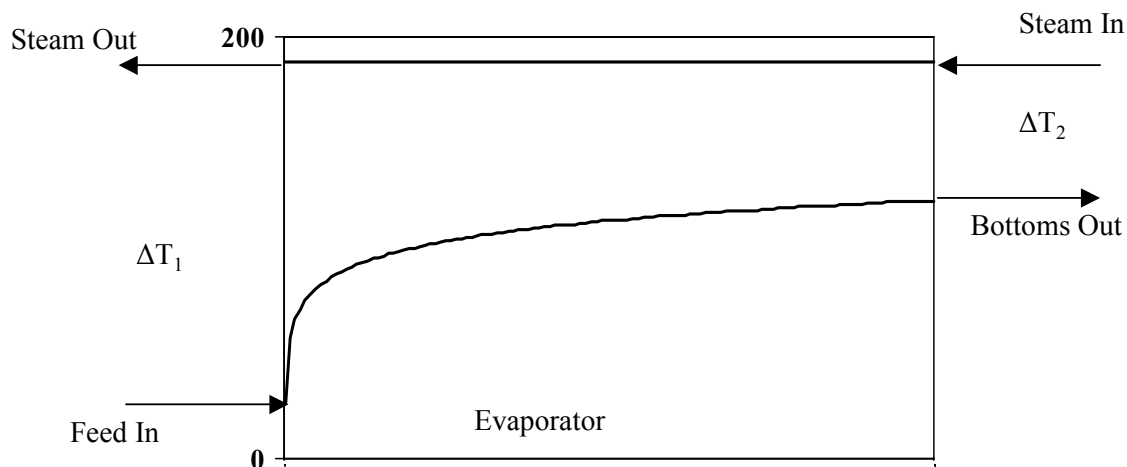


Figure 12. Conceptual graphic of the log-mean temperature difference used to calculate energy balance.

The energy balance was calculated based on the assumption that the distillate leaving the evaporator was 100% vapor and the bottoms leave the evaporator as an aqueous solution. When calculating the evaporator heat duty for the first series of ATFE tests, it was demonstrated through a sensitivity analysis that the result is not significantly affected by reasonable changes in these assumptions.⁵ The calculated energy balance for each run is summarized in Table 10. The heat transfer coefficients in Table 10 are about 8% lower, on average, than those calculated for the second series of tests.

Table 10. Calculated energy balance for each ATFE pilot-scale run.

Run	Temperatures, °C					Log-mean temp. difference	Required Heat Input, Watts	Overall heat transfer coef., W/m ² /K
	Feed	Bottoms	Vapor	Steam in	Steam out			
AL-1-1	31.3	119.8	97.7	179.9	179.1	96.9	20,138	1598
AL-1-2	29.8	120.1	97.6	180.0	179.2	97.4	20,187	1594
AL-2-1	27.3	127.2	99.0	187.9	187.0	101.7	21,849	1652
AL-2-2	29.0	128.0	99.3	187.7	186.8	100.3	22,068	1692
MG-1-1	30.0	129.0	99.5	188.4	187.4	99.9	22,780	1754
MG-1-2	30.9	124.1	99.4	188.4	187.4	103.0	21,363	1595
MG-2-1	28.3	131.5	96.5	193.7	192.8	104.5	21,815	1604
MG-2-2	29.6	132.4	96.9	193.7	192.8	103.4	22,580	1679

4.2 Control of Evaporator Bottoms Concentration

As in previous tests, bottoms concentration was controlled by establishing a constant feed rate and then adjusting steam pressure/temperature to achieve the desired condensate production rate during the aluminum tests. Once the desired split was achieved, concentrated bottoms material was collected in a

15-gal drum. However, this method used up an undesirable quantity of feed. As a result, the second 15-gal drum was only filled about halfway before the high aluminum feed was depleted. Consequently, a new strategy was employed for the magnesium tests.

The target concentration for the first magnesium test was 55 wt% of the feed evaporated. During the first aluminum test, 54 wt% evaporated resulted in a bottoms temperature of 120 °C. Thus, for the first magnesium test, steam pressure was increased until the bottoms temperature reached 121.5 °C. Then collection of bottoms in the 15-gal drum was initiated. The fraction evaporated was determined to be about 52 wt%, so the steam pressure was increased, producing a higher bottoms temperature. Adjustments were made as needed throughout the test to achieve the desired bottoms concentration. The same strategy was used for the second magnesium test. Figure 13 charts the fraction of feed evaporated versus bottoms temperature to illustrate the test results.

This control strategy would work better in a production facility than it did in the pilot plant. A vessel large enough to hold the condensate produced while filling a single waste container could be used. Monitoring the level and density in the condensate vessel would make it possible to continuously monitor the rate of condensate production. In contrast, a minimum of 6 minutes was required for each condensate rate check in the pilot plant, and there was always significant elapsed time between rate checks.

4.3 Fouling of Heating Surface

As in previous tests, there was no evidence of fouling. This is significant because continuous run times were longer during the third test series compared to previous series. Energy balance data were collected for each test condition twice with 2 to 6 hours of time elapsed in between. An overall heat transfer coefficient was calculated for each case (see Table 10). Overall heat transfer coefficients did not change significantly over time. For example, the final test condition was a feed based on overhead recycle neutralized with magnesium and approximately 62 wt% of the feed evaporated. The overall heat transfer coefficient after 2 hours of operation was 1550 W/m²/°C. The overall heat transfer coefficient after nearly 7 hours of operation was 1620 W/m²/°C.

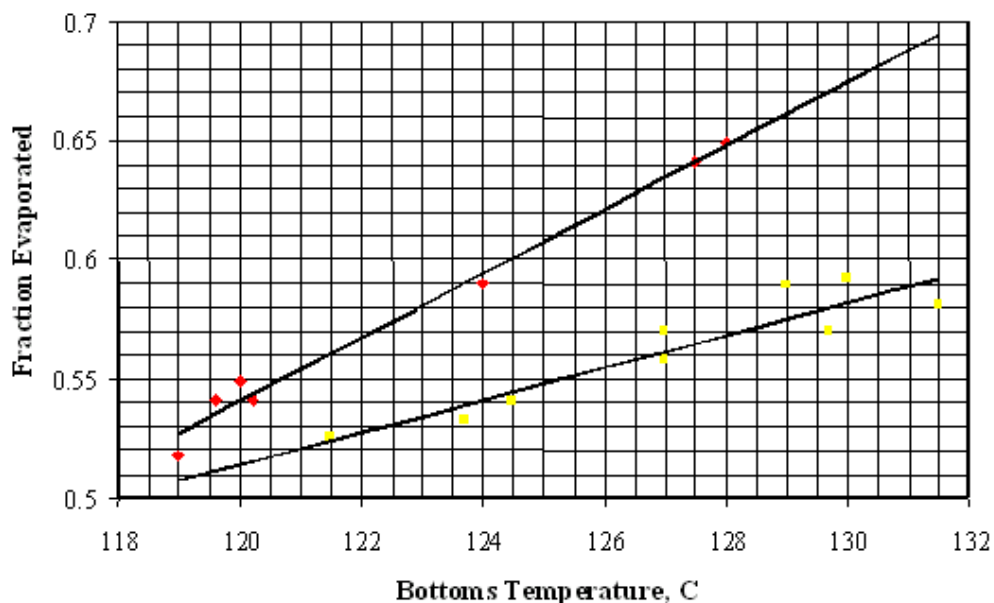


Figure 13. Feed fraction evaporated versus bottoms temperature.

Besides the fact that the heat transfer coefficient did not change while maintaining constant conditions, the heat transfer coefficients did not vary significantly throughout approximately 25 hours of testing. The evaporator was rinsed briefly with feed solution immediately prior to each shutdown, but the purpose was to flush concentrate from the evaporator and not to mitigate fouling.

The rotor was pulled and the inside of the evaporator was inspected during the third test condition, after the third test condition, and after the final test. The evaporator walls were clean.

Although there was no indication of fouling in any of the tests with simulated SBW, the possibility of fouling with actual SBW cannot be ruled out. The simulant only contained major chemical components. Low concentrations of silicates or carbonates found in the actual SBW might contribute to fouling.

4.4 Plugging of Bottoms Discharge

The bottoms material flowing from the evaporator appeared to be less viscous for this test series than in previous tests in which the feed did not contain as much aluminum or magnesium. (Figure 14). However, the material appeared to solidify more quickly. Both observations were most obvious for the more concentrated bottoms produced from the high aluminum feed in Run AL-2. AL-2 is shown in Figure 15.

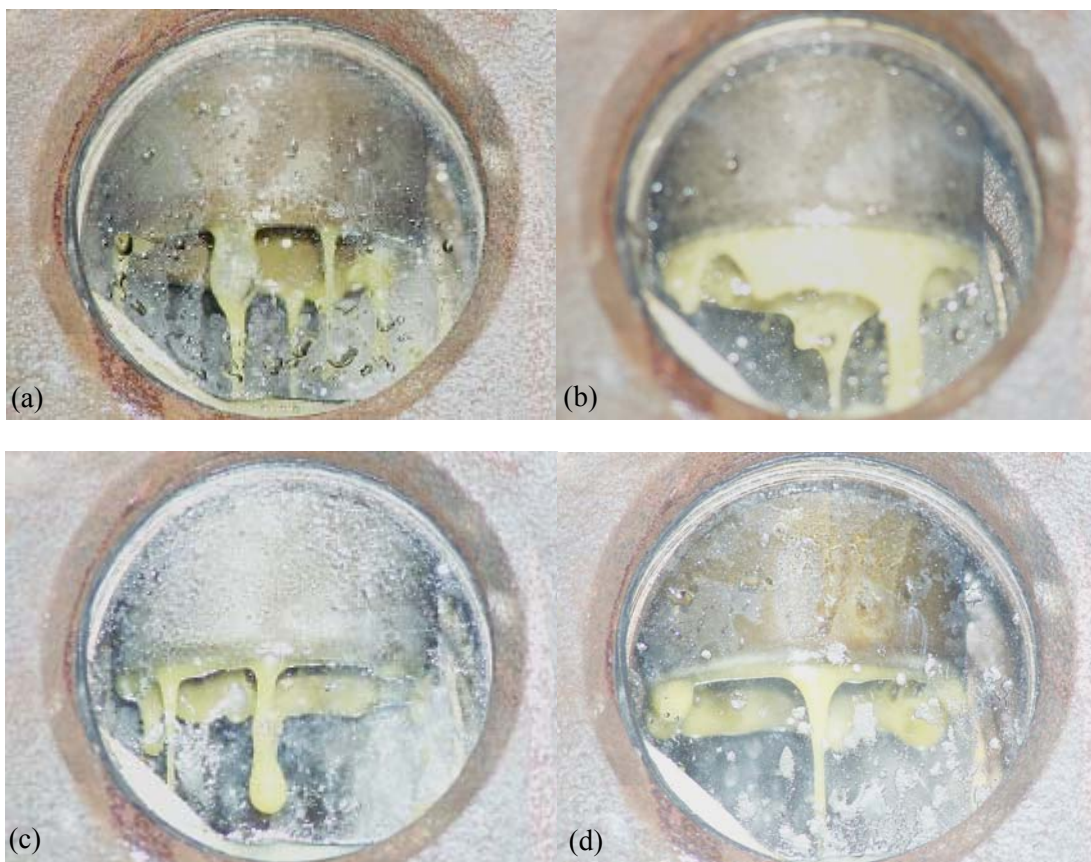


Figure 14. Evaporator bottom discharge for the high aluminum feed at 54.7 wt% (a) and 62 wt% (b) and for the high magnesium feed at 54 wt% (c) and 61 wt% (d).



Figure 15. View of the AL-2 (62 wt%) bottoms leaving the timed discharge vessel.

The evaporator bottom discharge plugged during the first high magnesium test after 3-1/2 hours of operation. This was the only time the evaporator bottom plugged. Most likely, the plug was caused by solidified material hung up in the evaporator from the final high aluminum test. The initial high magnesium bottoms material was not so highly concentrated that it would have been likely to cause a problem. In comparison, the final high aluminum material was very concentrated and slow to dissolve once it was solidified. The day after the plugging incident, the evaporator was operated for 7 hours and 20 minutes with higher bottoms concentration, and the bottom discharge did not plug.

The first indication of the bottom plug was accumulation of liquid in the flask attached to the demister drain and no flow from the evaporator bottom discharge. Rotor current increased from 2.0 to 3.0 amps. No vibrations were noted.

When evidence of the bottom plug was first noted, the feed, steam, and rotor were immediately shut off. An attempt was made to clear the evaporator bottom discharge by applying backpressure with nitrogen in the timed discharge vessel. This did not work, so the evaporator rotor was removed. The bottom foot of the evaporator was packed with solid concentrate (see Figures 16 and 17). However, there was no sign of fouling on surfaces above this accumulation. The evaporator was rodded out from above. The solid material was soft, but it would not flow by gravity past the spokes that center the bottom bearing, so it had to be pushed through.

There was one evaporator bottom-plugging incident during the first test series while feeding WM-189 simulant. The plug was believed to have started in the view port immediately below the evaporator discharge. Simply shutting off the steam allowed the feed that had accumulated in the evaporator to dissolve that plug in a few minutes.

Recovery from a bottom plug in a production evaporator could be much more costly, because hands-on removal of the rotor or manual rodding out would be prevented by radiation. The preferred approach would be to dissolve the plug with acid. Plugs may be less likely in a production facility,



Figure 16. Evaporator rotor with buildup of bottoms.



Figure 17. Inside evaporator vessel after discharge plugged.

because (1) the process would be operated more conservatively, (2) the evaporator would be larger and less prone to plugging, and (3) the system would be specifically designed for this process. In contrast, the pilot plant is designed for versatility and has a more complicated discharge system and a less responsive control system than may be required for processing SBW.

The evaporator bottoms plugging incident demonstrates the importance of a good strategy for controlling bottoms concentration. It also indicates some important design issues. Generally, the simpler the bottom discharge is, the less likely it will be to plug. However, if it does plug, a method will be needed to clear the plug remotely.

Although evaluation of the evaporator was not a primary objective of this test, the flow characteristics of the bottoms material are only applicable to the ATFE. An evaporator that provided longer residence time and less agitation would be expected to produce larger crystals as seen in flask-scale tests. This would result in a liquid phase with relatively low viscosity compared to the sludge produced in the ATFE, and crystals with high settling rates.

4.5 Waste Form Properties

4.5.1 Flask-Scale Tests

The feed volume/mass reductions attained during the flask-scale tests are summarized in Table 11. The nominal vacuum for each of these tests was 254 mm Hg for FSR-1 (Na), FSR-3 (Al), and FSR-5 (Mg) and 254 to 381 mm Hg for FSR-2 (Na), FSR-4 (Al), and FSR-6 (Mg).

The magnesium recycle flowsheet could not be concentrated past approximately 59 wt% by the flask-scale system. The highest concentration attained for the sodium flowsheet was approximately 59 wt% reduction, which resulted in a sugary product of liquid filled with sodium nitrate crystals with a little liquid which could not be poured into a separate container. Not all of the first Na run bottoms could be poured from the flask either. About 20% remained with the flask and had to be washed out. In a full-scale, continuous process, this would result in plugging of the bottoms discharge from the evaporator, an undesirable outcome. The aluminum recycle flowsheet yielded the highest volume and mass reductions.

Table 11. Waste form data for the flask-scale tests.

Flask Run	End Point Temp. Solution, °C	Wt% Mass Reduction	Wt% Mass Reduction – SBW Feed Basis	% Volume Reduction	% Volume Reduction – SBW Basis	Wt% H ₂ O in Product
FSR-1 (Na)	114.4	56.35	45.11	67.31	54.48	22.47
FSR-2 (Na)	113.8	60.89	50.53	70.54	58.98	17.82
FSR-3 (Al)	126.4	56.74	44.88	67.87	55.26	27.57
FSR-4 (Al)	122.5	68.26	59.45	75.85	66.38	18.18
FSR-5 (Mg)	125.3	57.82	47.18	68.93	56.74	31.13
FSR-6 (Mg)	123.6	59.21	48.91	70.13	58.41	31.62

4.5.2 Pilot-Scale Tests

4.5.2.1 Bottoms Composition. The bottoms composition, summarized in Table 12, was determined from the difference between the feed and distillate compositions.

In general, the bottoms produced with the overhead recycle feed were less viscous prior to cooling than previous feeds. However, the bottoms tended to solidify more quickly, especially for the high aluminum feed (aluminum recycle), see Figures 14 and 15.

4.5.2.2 Volume Reduction. The volume evaporated for each run is presented in Table 13. This is expressed both as a percent of evaporator feed and as a percent of the SBW that would have been processed. Overhead recycle increased the feed volume by about 25% based on the assumptions stated in Section 2. One of these assumptions—the concentration of acid fractionator bottoms—would not be expected to affect the volume evaporated as a fraction of SBW processed. For example, increasing the concentration of fractionator bottoms would slightly increase the concentration of evaporator feed, but the feed would still be evaporated to the same final bottoms concentration. The other assumption—the percent of acid evaporated—would affect overall volume reduction. Overall volume reduction would decrease slightly if more acid was evaporated. The fact that the percent of acid evaporated was consistently higher than the assumed 85% implies that the overall volume reduction presented in Table 13 might not be achieved by the proposed flowsheet.

The weight percent of the feed evaporated was recorded for each run as described in Section 4.1, Table 8. The bulk density of the solidified bottoms was determined by measuring the amount of water displaced by a known mass of bottoms. This method appeared to be as accurate as the graduated cylinder used to measure the water. There was a concern that water would gradually soak into the pores of the solids and the solids would go into solution. However, no change in the volume was detected in the time required to obtain the total mass of graduated cylinder, bottoms, and water. The results compared well to the bulk densities measured in the past by other methods. The best method would be to pour bottoms material into a calibrated container before it solidifies.

Table 12. Bottoms composition, in weight percent, for the ATFE pilot-scale runs.

	AL-1-1, wt%	AL-1-2, wt%	AL-2-1, wt%	AL-2-2, wt%	MG-1-1, wt%	MG-1-2, wt%	MG-2-1, wt%	MG-2-2, wt%
Cesium	5.00×10^{-3}	5.00×10^{-3}	6.00×10^{-3}	6.00×10^{-3}	5.00×10^{-3}	4.00×10^{-3}	5.00×10^{-3}	5.00×10^{-3}
Aluminum	5.63	5.63	6.83	6.98	2.55	2.34	2.76	2.95
Calcium	0.34	0.34	0.41	0.42	0.39	0.36	0.42	0.45
Iron	0.18	0.18	0.22	0.23	0.21	0.20	0.23	0.25
Magnesium	0.07	0.07	0.08	0.08	4.07	3.74	4.42	4.72
Manganese	0.14	0.14	0.16	0.17	0.14	0.13	0.15	0.16
Potassium	0.98	0.98	1.19	1.22	1.31	1.20	1.42	1.52
Sodium	5.66	5.66	6.86	7.01	6.69	6.15	7.26	7.75
Sulfate	0.46	0.46	0.56	0.57	0.52	0.48	0.56	0.60
Nitrate	54.88	54.28	55.96	56.20	52.39	51.68	53.64	55.00
Water	31.67	32.28	27.91	27.33	31.82	33.76	29.30	26.80
Total	100.00	100.00	100.00	100.00	100.00	100.00	100.00	100.00

Table 13. Volume reduction data for the pilot-scale runs.

Run	Wt % Evaporated	Bulk Density g/mL	Volume Evaporated	
			% Evap. Feed	% SBW Processed
LCI#3				
AL-1-1	53.9	1.65	62.1	49.7
AL-1-2	53.9	1.65	62.1	49.7
AL-2-1	62.0	1.81	71.5	57.2
AL-2-2	62.8	1.71	70.5	56.4
MG-1-1	57.9	1.76	67.4	54.3
MG-1-2	54.1	1.70	63.2	51.0
MG-2-1	61.2	1.74	69.6	56.1
MG-2-2	63.6	1.86	73.3	59.1
LCI#2				
1 ^a	58.1	1.74	68.5	68.5
2 ^a	60.6	1.71	69.9	69.9
4 ^a	64.7	1.63	71.6	71.6
5 ^b	55.1	1.75	64.6	Not calculated
6 ^b	57.5	1.84	68.3	Not calculated
7 ^b	61.5	1.79	70.4	Not calculated
10 ^c	58.9	1.74	67.5	Not calculated
13 ^d	62.6	1.57	67.2	Not calculated
16 ^e	62.2	1.70	69.4	Not calculated
a. WM-189 with no tank heel solids surrogate.				
b. WM-189 with tank heel surrogate – 5wt% 2μm.				
c. WM-189 with tank heel surrogate – 5wt% 5μm silica.				
d. WM-189 with tank heel surrogate – 5wt% kaolin clay.				
e. WM-189 with tank heel surrogate – 5wt% Zr(PO ₄) ₂ .				

The average volume reduction from the second test series (see LCI#2 data in Table 13) was 70% for cases that did not contain insoluble material. That means that a volume of 378.5 L of SBW would produce 113.6 L of RH-TRU. In comparison, the overhead recycle flowsheet would result in 177.9 L of RH-TRU based on the average volume reduction for Runs MG-1 and MG-2, which is an increase of 56%. These runs were chosen for comparison, because they represent the most likely flowsheet for production. The volume increase between SBW and SBW with overhead recycle is dependent on the acid concentration in the SBW. WM-189 has a higher acid concentration than the other tanks at 2.8 M. WM-180 has the lowest at 1.0 M acid, so the increase in RH-TRU volume for WM-180 with overhead recycle would be lower, probably in the 20% range.

4.5.2.3 Bottoms Product Cooling (Stabilization). Thermocouples were placed at the centerline and approximately 1.25 in. from the drum side and located approximately midway up the drum. The thermocouple connector plugs in the solidified product can be observed in the photographs presented in Figures 18 and 19. Temperature profiles were collected for each drum during solidification and cooling. Drums were allowed to cool at room temperature (20–26°C) in the test facility with no specific control of air velocity or air temperature. The test room was well ventilated.

The photograph in Figure 20 is of Drum 1, which is the product of the aluminum recycle run with a 55% mass reduction. The product is very hard and fine-grained in texture. The photograph was taken approximately 2 months after the product was made. No free liquid was observed in the product after initial solidification had occurred. The top surface of the product appears to have developed a crust and is slightly risen in the center. Note also in the photograph that the connector terminals of the thermocouple connector plug are significantly corroded. No visible corrosion of the stainless steel drum, drum lid seal, or bung seals was observed.



Figure 18. Thermocouples in first drum for the high aluminum feed and 54.7 wt% evaporated.



Figure 19. Thermocouples in drum with high magnesium feed and 55 wt% evaporated.



Figure 20. Photograph of solidified surface layer of Drum 1; aluminum recycle at 55% mass reduction.

The photograph in Figure 21 is of Drum 3, which is the product of the magnesium recycle run with a 55% mass reduction. The product is very hard and appears to have a combination of larger crystals and fine-grained crystals on top. The photograph was taken approximately 2 months after the product was made. No free liquid was observed in the product after initial solidification had occurred. The mechanisms that allowed the large crystal growth were not observed. The top surface of the product appears to have subsided during cooling as the center is lower than the edges. Note also, similarly to the aluminum product, that the connector terminals of the thermocouple connector plug are significantly corroded. No visible corrosion of the stainless steel drum, drum lid seal, or bung seals was observed.

The drum temperature profile and temperature gradient between thermocouples during the solidification and cooling of Drum 1 are illustrated in Figure 22. Drum 1 is the product material of the aluminum recycle run with a 55% mass reduction. Note that a temperature gradient quickly developed between the inside and outside thermocouple, which is what would be expected since most of the heat



Figure 21. Photograph of solidified surface layer of Drum 3; magnesium recycle at 55% mass reduction.

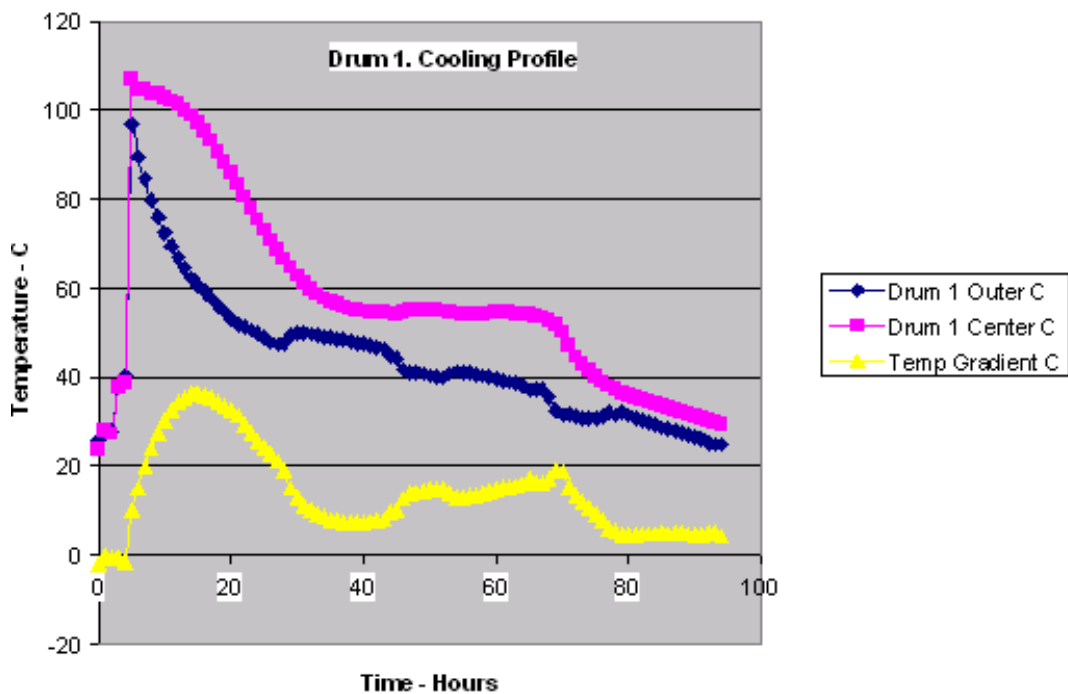


Figure 22. Cooling temperature profile for Drum 1.

would dissipate radially to the outside surface. After the initial development of the temperature gradient, the gradient declines as would be expected, due to reduced heat transfer at the outer surface of the drum (less temperature gradient between the drum surface and ambient air; therefore, less heat transfer). At approximately 40 hours into the cooling cycle the temperature gradient again becomes larger; coincidentally, the centerline temperature stabilizes and remains essentially constant for approximately 30 hours. At the time that the centerline temperature starts dropping again the temperature gradient declines and the product cools as would be expected. Similar behavior was observed in the first ATFE test

series. When monitoring the temperature in the center of the 5-gal bucket of evaporator bottoms, the temperature dropped initially, but then increased for a period of time.

The cooling curves may be explained by heats of reaction. Just as Portland cement generates heat as it hydrates, the transition from aluminum nitrate hexahydrate to aluminum nitrate nonahydrate has an exothermic heat of reaction of 49 kJ/mole. In Figure 22, the centerline temperature of Drum 1 is level for about 40 hours at over 50°C. This drum contains about 200 moles of aluminum. Assuming that every mole of aluminum made the transition over a period of 40 hours, the average heat generation rate would be over 60 W.

Most of the aluminum nitrate discharges from the evaporator in an aqueous form. The heat of crystallization in forming aluminum nitrate hexahydrate is an endothermic 19 kJ/mole. Thus, crystallization probably increases the cooling rate initially for high aluminum bottoms.

The drum temperature profile and temperature gradient between thermocouples during the solidification and cooling of Drum 2 are illustrated in Figure 23. Drum 2 is the product material of the aluminum recycle run with a 65% mass reduction. Note that, similarly to Drum 1, a temperature gradient quickly developed between the inside and outside thermocouple. After the initial development of the temperature gradient, it declines as would be expected. As observed in Drum 1, a perturbation of the temperature gradient is observed at approximately 25 hours into the cooling cycle; however, with Drum 2 it is much less pronounced. Note also that at approximately 40 hours into the cooling cycle the inner and outer thermocouple temperatures have nearly converged. Shortly thereafter, the centerline temperature increases and then finally reconverges with the outer temperature. This observation would be consistent with an exothermic reaction occurring at approximately 40 hours into the cooling cycle.

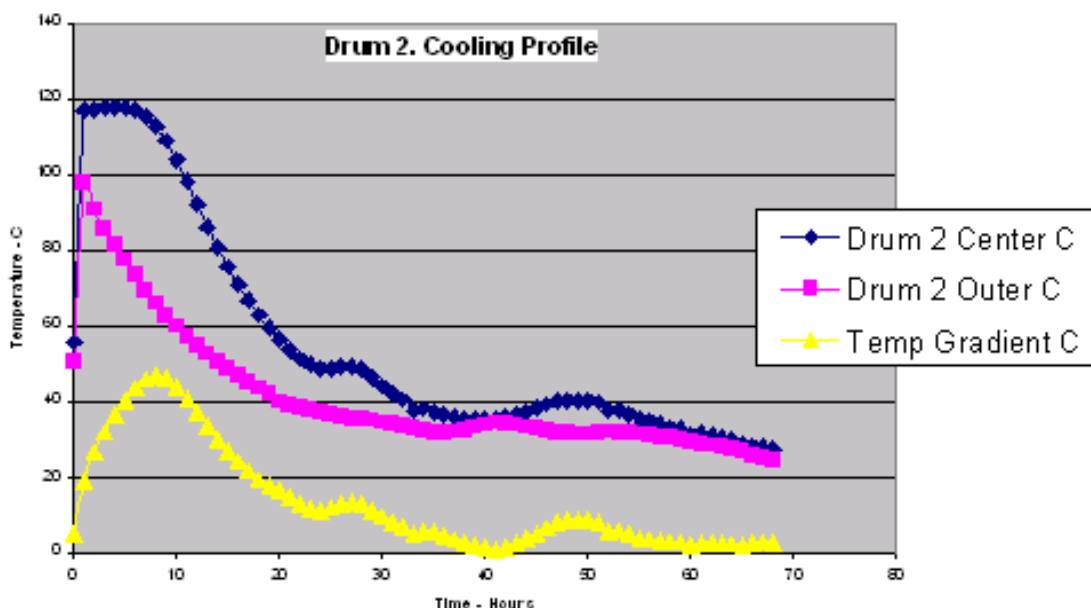


Figure 23. Cooling temperature profile for Drum 2.

The product resulting from 65% mass reduction (Drum 2) does not contain enough residual water that all of the aluminum nitrate can exist in the nonahydrate state. This would contribute to the difference in the cooling temperature profiles of Drum 1 and Drum 2. It would be expected that product derived from the same feed materials would be very similar. The water content and a small change in the acid content are the only differences between Drum 1 product and Drum 2 product compositions. Another important difference between the two drums is that Drum 2 was only half full.

The cooling profile for Drum 3 is illustrated in Figure 24. Drum 3 is the product material from the magnesium recycle test iteration at 55% mass reduction. Drum 3 cooled much more slowly than Drums 1 and 2. For Drum 3, the temperature gradient quickly develops and then remains relatively constant, but slowly drops as the drum contents cool. The centerline temperature appears to remain constant during the time interval of 35 to 45 hours. Magnesium nitrate dihydrate and hexahydrate have higher melting or transition points than the aluminum nitrate compounds. The high magnesium bottoms material was more viscous than the high aluminum bottoms at the evaporator discharge indicating that more of it was crystallized. Clearly, the net reactions occurring initially in the drum were exothermic. The heat of reaction for converting aqueous magnesium nitrate to magnesium nitrate hexahydrate is an exothermic 21.3 kJ/mole. The heat of reaction for converting magnesium nitrate dihydrate crystals to hexahydrate is also exothermic at 60.8 kJ/mole. Only the conversion of aqueous to dihydrate is endothermic. The cooling curves indicate that this reaction was either nearly complete when temperature monitoring was initiated or that the transition from dihydrate to hexahydrate occurred at a relatively high rate.

Even though magnesium is used as the neutralizing agent, there is a significant mass of aluminum in the product from the SBW surrogate. This aluminum is available to form aluminum nitrate nonahydrate provided water is available. At 55% mass reduction there is stoichiometrically adequate water for this to occur. It is likely that the centerline temperature stabilization occurring during the time interval of 35 to 45 hours is related to the hydration of aluminum nitrate hexahydrate as postulated for Drum 1.

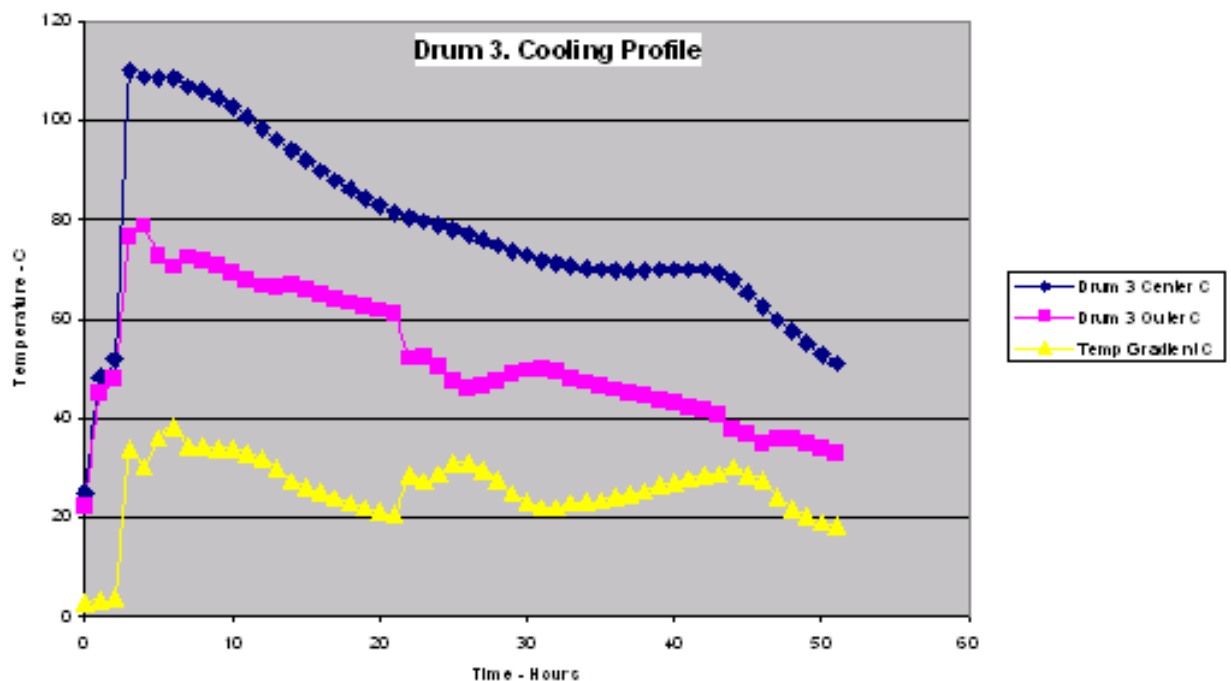


Figure 24. Cooling temperature profile for Drum 3.

The cooling profile for Drum 4 is illustrated in Figure 25. Drum 4 is the product material from the magnesium recycle test iteration at 62% mass reduction. The cooling profile is similar to Drum 3 with two notable differences. The first difference is that the temperature gradient between Drum 4 thermocouples is approximately half of that observed for Drum 3. The second is that the centerline temperature continually and uniformly declines over the whole cooling cycle. The cooling profile observed in Drum 4 is similar to what would be expected for a uniform solid material with a constant thermal conductivity.

As with Drum 2, the product contained in Drum 4 does not contain enough water to fully hydrate all of the salts. This could explain the apparent lack of an exothermic reaction during the cooling cycle.

From the four cooling profiles presented in this report, it is apparent that the neutralizing agent and the extent of evaporation both have a significant influence on the cooling properties of the direct evaporation product. It is also apparent that cooling of a waste container using air heat transfer will be much slower than waste container filling.

4.5.2.4 Scalability of Heat Transfer and Modeling. The 15-gal bottoms drums used for this test were 14.7 in. in diameter. Actual RH-TRU canisters have an inside diameter of 25.5 in. This will result in much slower cooling. For a given bottoms material there will be three times more material per unit height in a full-scale container. This means there will be three times as much sensible heat and heat of reaction to dissipate. In addition, bottoms material is not a particularly good conductor, so increasing the diameter of the container may be akin to adding insulation. Ignoring heat of reaction and using curves for one-dimensional cooling of an infinite cylinder, it was estimated that a full-scale waste container would take about five times as long to cool. This scale-up factor depends on the relative resistance, which is calculated from the ratio of thermal conductivity to convective heat transfer coefficient. Although precise values are not available, the result does not appear to be very sensitive over the range of reasonable values.

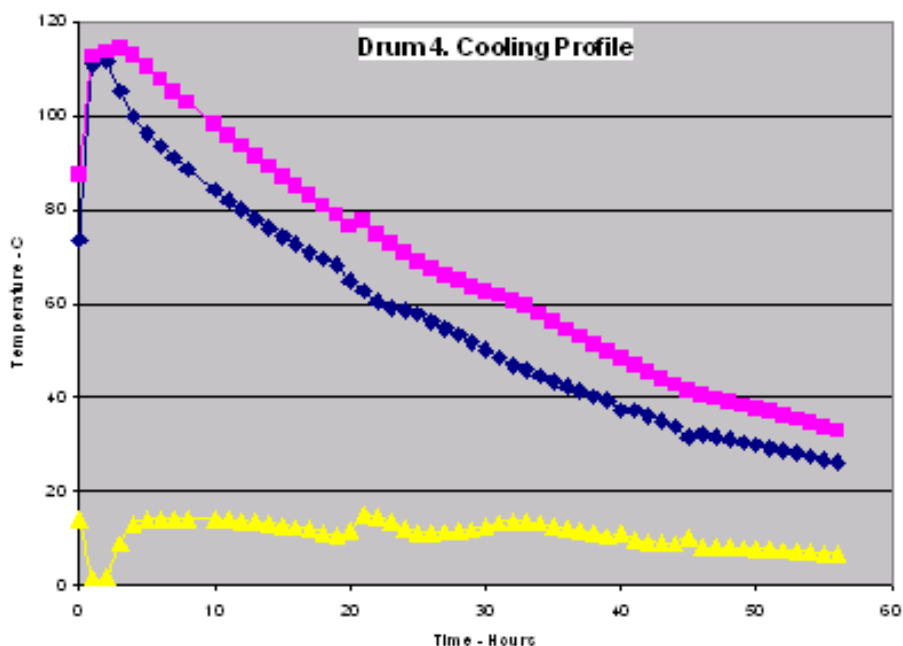


Figure 25. Cooling temperature profile for Drum 4.

The possibility of using the cooling curves to create a computer model of container cooling should be considered. One approach would be to use finite element analysis. Beginning with reasonable estimates for heat capacity, thermal conductivity, and convective heat transfer coefficient, it may be possible to tune the model to match the cooling curves by varying the reaction rates using reasonable assumptions for the affect of temperature. A model that matches the 15-gal drum cooling curves could be scaled to provide a good estimate of the time required for cooling a full-scale container.

4.5.2.5 Bottoms Product Expansion After Cooling (Stabilization). On a few occasions during prior tests of direct evaporation, it was observed that the evaporator product may have expanded on cooling. In several cases, glass containers have cracked and it was theorized that expansion of evaporator product caused the failure. In the second series of ATFE tests, 5-gal plastic buckets of bottoms expanded, especially the top layer of material. An attempt was made during these tests to quantify expansion of the product upon solidification. To complete this evaluation, each product drum was marked at seven locations and the diameter of the drum was measured before product was cast in the drum. After the product drums were solidified and cooled, diameter measurements were taken again. All measurements were made with a pi-tape, which is certified accurate to ± 0.0025 cm. It would require controlled conditions and a trained eye to achieve that accuracy, but ± 0.005 cm was probably realistic for this effort. The measurements are presented in Table 14.

Based on the dimensional observations presented in Table 14, there is evidence that expansion of the aluminum surrogate at 55% mass reduction does occur. This is consistent with the physical observation that the top surface of the material appeared raised.

Table 14. Physical drum dimensions before product loading and after solidification.

Drum # 1, Aluminum Neutralization At 55% Mass Reduction (drum diameter measurements in inches)

From Top (in.)	Before Run 11/07/03	After Run 12/09/03	Difference	After Run 1/15/04	Difference
1	14.031	14.030	-0.001	14.032	0.001
2	14.037	14.032	-0.005	14.033	-0.004
3	14.036	14.053	0.017	14.053	0.017
4	n/m	n/m	n/m	n/m	n/m
5	14.033	14.080	0.047	14.083	0.050
12	14.033	14.134	0.101	14.140	0.107
22	14.035	14.113	0.078	14.116	0.081
Average difference			0.040		0.042

Drum # 2, Aluminum Neutralization At 65% Mass Reduction (drum diameter measurements in inches)

From Top (in.)	Before Run 11/07/03	After Run 12/09/03	Difference	After Run 1/15/04	Difference
1	14.030	14.028	-0.002	14.030	0.000
2	14.037	14.038	0.001	14.041	0.004
3	14.033	14.032	-0.001	14.037	0.004
4	14.035	14.038	0.003	14.036	0.001
5	14.028	14.032	0.004	14.032	0.004

Table 14. (continued).

12	14.029	14.030	0.001	14.030	0.001
22	14.035	14.048	0.013	14.046	0.011
Average difference			0.003		0.004
Drum # 3, Magnesium Neutralization At 55% Mass Reduction (drum diameter measurements in inches)					
From Top (in.)	Before Run	After Run	Difference	After Run	Difference
	11/07/03	12/09/03		1/15/04	
1	14.035	14.040	0.005	14.032	-0.003
2	14.037	14.032	-0.005	14.038	0.001
3	14.038	14.040	0.002	14.050	0.012
4	14.033	14.039	0.006	14.048	0.015
5	14.038	14.035	-0.003	14.048	0.010
12	14.039	14.050	0.011	14.053	0.014
22	14.035	14.040	0.005	14.037	0.002
Average difference			0.003		0.007
Drum # 4, Magnesium Neutralization At 62% Mass Reduction (drum diameter measurements in inches)					
From Top (in.)	Before Run	After Run	Difference	After Run	Difference
	11/07/03	12/09/03		1/15/04	
1	14.030	14.030	0.000	14.028	-0.002
2	14.029	14.028	-0.001	14.037	0.008
3	14.035	14.036	0.001	14.036	0.001
4	14.029	14.037	0.008	14.029	0.000
5	14.028	14.031	0.003	14.029	0.001
12	14.028	14.033	0.005	14.029	0.001
22	14.035	14.029	-0.006	14.039	0.004
Average difference			0.001		0.002

4.6 Waste Form Critical Parameters Assessment

4.6.1 Radiological Properties

Previous modeling work generated detailed mass balances of several SBW flowsheets in a direct evaporation process.⁸ The model assumed an SBW feedrate of 335 L/hr with an evaporator bottoms production rate of 134 L/hr for a 60% volume reduction. Approximately 100% of the radioisotopes in the SBW partitioned to the bottoms product. The radioisotope throughput in the system was calculated at 73.5 Ci/hr. From this information, the TRU alpha activity in an RH-TRU canister was estimated, assuming that the canister is filled to 800 L and the mass of the canister does not need to be added into the calculation. The activity estimate was 313,400 nCi/g, and the maximum activity averaged over the canister volume is approximately 0.6 Ci/L. Both of these estimates are well within the limits established

by WIPP (>100 nCi/g and <23 Ci/L). The same calculations were completed to evaluate the pilot-scale test data from evaporation of an SBW surrogate. The same SBW feedrate and radioisotope concentrations were assumed (335 L/hr and 73.5 Ci/hr). The calculations are summarized in Table 15. In the absence of real waste data, an absolute determination that the evaporated SBW with recycle waste form meets the radiological properties requirements for the transport and disposal of RH-TRU waste cannot be made. However, based on these simple calculations it appears likely that the waste form would meet at least two of the radiological properties requirements for the transport and disposal of RH-TRU waste at WIPP.

4.6.2 Hydrogen Generation and Total Gas Limits

Actual gas generation rates will be difficult to determine until real waste tests are completed. Until that time, evaluation of the waste form against the 72B shipping cask's hydrogen generation and total gas limits is theoretical. Previous work generated a model that predicts hydrogen gas generation rates from evaporated SBW with various water contents. Evaporator bottoms product with water content less than 20 wt% should not exceed the hydrogen gas generation limits for the 72B. However, the calculated water content in the pilot-scale evaporator product was 27–33 wt% water based on the difference between the feed and distillate. The water content of the waste form after cooling and solidification may be less than this difference. Future tests of the final waste form should include analysis for water in the solidified waste form. The nitrates in the waste form could prevent the maximum allowable hydrogen gas generation rate from being exceeded; however, gas generation testing on the real waste is necessary to predict with certainty that the waste is shippable.

Experimental work has also demonstrated that the bottoms product continues to off-gas after cooling. This is discussed in detail in Section 4.6.3. Additional testing should be completed to determine the quantity of off-gas produced and ensure that it is below the 72B shipping cask's total gas limits.

Table 15. Theoretical calculations to determine TRU activities.^a

	% Volume Reduction	Bottoms Volume (L)	Bottoms Density (kg/L)	Bottoms Weight (kg)	TRU Activity (nCi/g)	Total Activity/ Canister (Ci)	Activity Level (Ci/L)
Theory	0.6	134	1.75	234	313,400	438	0.49
AL-1-1	0.5	167.5	1.65	276	265,900	351	0.39
AL-1-2	0.5	167.5	1.65	276	265,900	351	0.39
AL-2-1	0.57	144.05	1.81	260	281,900	408	0.46
AL-2-2	0.56	147.4	1.71	252	291,600	399	0.45
MG-1-1	0.54	154.1	1.76	271	271,000	382	0.43
MG-1-2	0.51	164.15	1.7	279	263,400	358	0.40
MG-2-1	0.56	147.4	1.74	256	286,600	399	0.45
MG-2-2	0.59	137.35	1.86	255	287,700	428	0.48

a. Assumptions: 1 hour of process time, 335 L of SBW feed, 73.5 Ci in bottoms, 800 L of waste per canister, total canister volume of 890 L.

4.6.3 Chemical Compatibility

The thermocouples used to monitor cooling of the bottoms material prevented sealing the drum lid, but a large plastic bag was taped in place over the top of each drum, minimizing emissions from the bottoms material to the atmosphere while cooling. The plastic bags never appeared to be pressurized or even partially filled with vapor. Once recording of bottoms cooling data was completed, the thermocouple wires were removed from the drums and the drum lids were sealed.

Gas samples collected from the headspace of the 15-gal drums were evaluated for NO_x using Drager tubes. Initial readings were taken shortly after the drums were filled and still cooling. The drums were then shipped from Charlotte, North Carolina, to INTEC. At INTEC, the drum lids remained sealed while monitoring NO_x concentration in the headspace of each drum. The small bung was periodically removed from each drum for a NO_x measurement. Results of these initial NO_x readings are shown in Figure 26 below. These levels would be influenced by the temperature and composition of the top layer of bottoms material. The second high aluminum drum was only half full, so the increased headspace may have affected NO_x levels. In all three drums, the NO_x concentration was trending downward. No measurements were obtained for the second high magnesium drum while cooling, because personnel were not available at that time.

After the bottoms drums were sealed and shipped to INTEC, NO_x levels were measured again several times and are presented in Table 16. The NO_x levels increased compared to the final measurements taken while the drums were cooling. Twice, the headspace of each drum was sampled and then purged with air to eliminate the NO_x. Within a few days, the NO_x levels returned to the previous values within the accuracy of the Drager tubes.^b This result indicates that the headspace becomes saturated with NO_x fairly quickly.

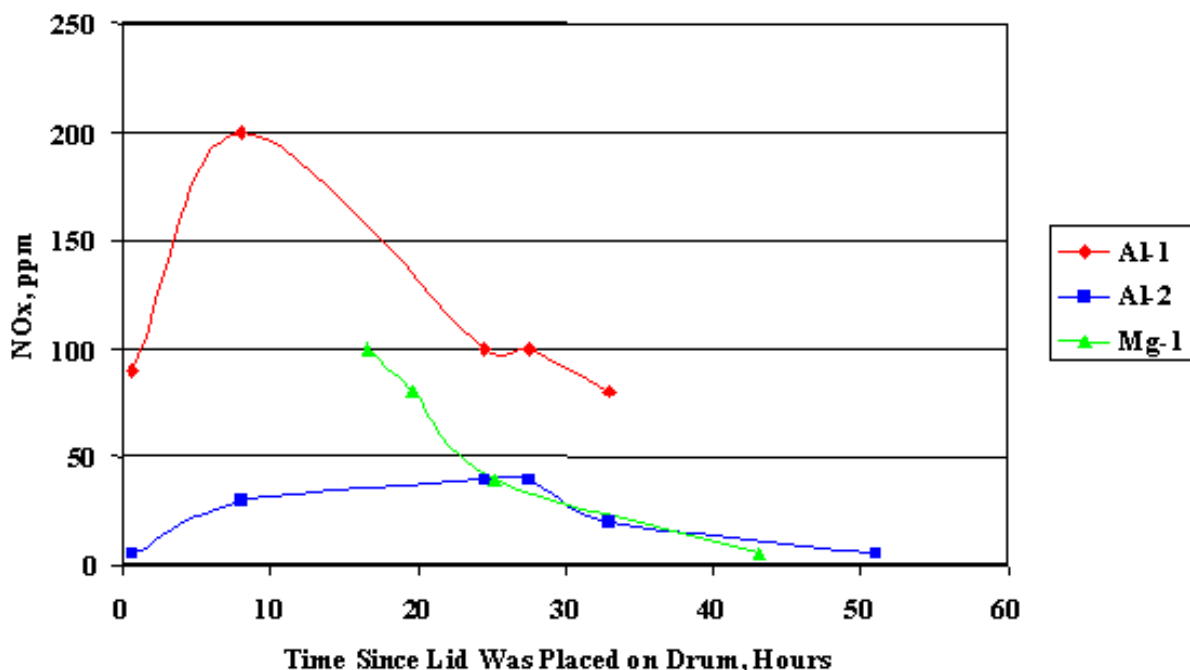


Figure 26. Drum headspace NO_x levels during cooling.

b. The manufacturer claims a standard deviation of 10 to 15%, but it would be difficult to achieve that level of precision with readings that are taken days apart.

Table 16. NO_x levels in headspace of cooled bottoms drums.

Drum	AL-1, ppm	AL-2, ppm	MG-1, ppm	MG-2, ppm
29 days after sealing drum lids	100	20	60	80
Immediately after first air purge of head space	0	0	0	0
13 days after first air purge	100	60	40	100
27 days after first air purge	100	60	40	80
Immediately after second air purge of head space	0	0	0	0
1 day after second air purge	40	5	7	12
2 days after second air purge	60	10	20	30
3 days after second air purge	100	20	40	80
6 days after second air purge	100	40	30	100
8 days after second air purge	100	40	60	100

When the drums were initially opened at INTEC, gas could be heard escaping as the bungs were loosened. This was due to pressure changes related to drum shipment—the drums were initially sealed at near sea level where the pressure was about 1.0 atm and the pressure at INTEC is only about 0.83 atm. No gas was heard escaping when the drums were subsequently opened. No measurements were taken, but the total vapor pressure of the bottoms material would be very low at ambient temperature.

Considering that NO_x is still present for a period of time after production, additional evaluation should be performed to determine the concentration at which NO_x in the headspace of the bottoms containers is an issue with respect to shipping and WIPP acceptance requirements. In previous tests, NO_x could not be identified in the bottoms product containers after approximately 6 weeks in a 19-L, ventilated container; therefore, it is likely that the waste form can be handled in such a fashion that it would meet this WIPP transportation and disposal criterion. Further tests may be necessary to determine appropriate NO_x mitigation solutions by either (1) identifying a waste canister stabilization period or (2) identifying an engineered solution. It is important to note that observed NO_x emissions eventually stop after a few days with small samples.

4.6.4 Corrosivity/Free Liquids

4.6.4.1 Flask-Scale Tests. With the exception of FSR-1 (Na), all of the waste forms appeared dry upon visual examination. Table 17 summarizes the results of the visual examination.

4.6.4.2 Pilot-Scale Tests. After 2 months of storage at INTEC, the drum lids (generated from pilot-scale tests) were removed to verify the absence of free liquids, see Figures 20, 21, 27, and 28.

Each waste form appeared dry to both a visual inspection and to the touch. There was no liquid present in any of the drums. The material clearly meets this waste acceptance criterion. Thus, for a waste form produced in an E/S process for SBW with magnesium- or aluminum-neutralized overheads recycle and with operating parameters similar to those used in these series of tests, the risk that it would fail to meet this transportation and disposal requirement is minimal.

Table 17. Visual examination results of the experimental waste forms from flask-scale tests.

Test #	Visual Examination Comments
FSR-1(Na)	Slurry of sugary-looking NaNO_3 crystals and the balance of the solution. Setup into a damp non-homogenous material that crumbled when disturbed,
FSR-2(Na)	Taken to a solid within the flask. Non-homogeneous.
FSR-3(Al)	At end point, the solution was crystal-free and poured easily. Setup into a homogeneous “rock” hard mass that was green in color.
FSR-4(Al)	Taken to a solid within the flask.
FSR-5 (Mg)	Product solution poured freely from the flask and setup into a “rock” hard, homogeneous product that was light red in color.
FSR-6 (Mg)	Product solution poured freely from the flask and setup quickly into an exceptionally tough ”rock” hard, homogeneous product that was light red in color. This was the hardest product out of all the lab tests.



Figure 27. Solidified product from SBW with magnesium-oxide-neutralized overheads pilot run – 62 wt% evaporated.



Figure 27. Solidified product from SBW with aluminum-hydroxide-neutralized overheads pilot runs – 62 wt% evaporated.

4.6.5 Ignitability

4.6.5.1 *Flask-Scale Tests.* The sodium recycle tests yielded a poor product with respect to this criterion. The FSR-1 test resulted in a crumbly, non-homogeneous product and the FSR-2 test also resulted in a non-homogeneous product. The magnesium and aluminum recycle tests resulted in bottoms products that were homogeneous, hard, and monolithic. Table 17 summarizes the results of the visual examination.

4.6.5.2 *Pilot-Scale Tests.* When the drum lids (generated from pilot-scale tests) were removed after 2 months cooling at INTEC, the physical appearance of the material was observed to determine if it was monolithic and non-friable. See Figures 20, 21, 27, and 28.

The examination to verify that the material is monolithic and non-friable is intended to demonstrate that the waste form would not have the EPA characteristic of ignitability. There are several ways waste forms in general could have this characteristic, but the concern with this waste form was that it might be classified as ignitable if it was a DOT oxidizer. The material would have to either be a powder or a liquid to be classified as a DOT oxidizer. There is a standard test to determine if a powder is a DOT oxidizer and it specifies that the “substance in the form in which it will be transported, should be inspected for any particles less than 500 μm in diameter. If that powder constitutes more than 10% (mass) of the total, or if the substance is friable, then the whole of the test sample should be ground to a powder before testing to allow for a reduction in particle size during handling and transport.” Otherwise, the procedure specifies that a powder be mixed with cellulose and tested “in the particle size in which it will be transported.”

From inspection of the drums after shipping and handling, it is clear that the material is not a powder, and it is not friable. There is some loose material on top of the second high aluminum drum, but it is not finer than 500 μm and it is much less than 10 wt% of the total. This drum was only half full and the loose material is concentrate that had adhered to the side of the drum and was knocked loose during transport.

It was concluded that additional testing using the DOT oxidizer Test Method 1040 would not be needed to qualify the test SBW with aluminum-neutralized and magnesium-neutralized overhead recycle waste forms as non-oxidizers.

5. CONCLUSIONS

- If an evaporator overhead neutralization and recycle flow sheet were implemented for the SBW in the INTEC tanks, magnesium oxide would be the best choice for a neutralizer. It is readily soluble in the overhead distillate (neutralization step) and produces evaporator bottoms material with desirable characteristics.
- The characteristics of evaporator bottoms prior to cooling and solidification are dependent on the evaporator. The flask tends to produce bottoms with relatively large crystals that readily settle in the liquid phase. The ATFE produces a viscous sludge consisting of fine crystals with interstitial liquid that has little or no tendency to separate into two phases. The difference in bottoms characteristics is attributed to the pronounced difference in residence time and agitation between the two evaporators.
- Cesium appears to be non-volatile at the evaporation temperatures used for these experiments, based on analysis of the overheads condensate. Cesium-137 is the source of nearly all of the penetrating radiation in the SBW; therefore, minimizing the cesium in the overheads will minimize the shielding requirements for overhead treatment and recycle.
- More acid evaporated to the distillate in the ATFE pilot plant than was assumed for calculating the initial SBW/recycle simulated waste feed composition. Consequently, the actual volume reduction will be less than indicated by the test results, because the acid in the distillate would all be neutralized and recycled.
- Emissions from direct evaporation will be minimal. This was demonstrated by the fact that essentially no secondary condensate was generated, which means there was very little non-condensable flow to carry water vapor past the primary condenser.
- Bottoms produced in the magnesium and aluminum recycle tests had acceptable flow characteristics and produced a non-friable, monolithic solid containing no free liquids.
- Although bottoms temperature provides a good indication of bottoms concentration, monitoring the distillate-to-waste/recycle feed ratio is the optimum strategy for controlling the bottoms concentration.
- Based on tests with this surrogate feed (i.e., simulated SBW/recycle), evaporator fouling is insignificant, and no adjustment to the existing evaporator process flowsheet for de-scaling is necessary.
- At full-scale evaporator operations, handling of the bottoms product will be an issue as demonstrated by the bottoms plugging incident during pilot-scale tests.
- Based on the pilot-scale results, direct evaporation with overhead neutralization and recycle will produce about a 53% volume reduction for WM-189 SBW. This results in about a 56% increase in RH-TRU volume when compared to direct evaporation without recycle. The increase would be less for the other SBW tanks wastes, since they have lower acid concentrations.
- The cooling times for pilot-scale-generated drums of bottoms product were significantly longer than the time to produce the material. The cooling curves also show the affects of exothermic

hydration reactions. Therefore, feasibility studies and cost estimates must take into account cooling and stabilization times.

- Since NO_x was still identified in the drum headspace above the bottoms product 2 months after production, additional evaluation must be performed to determine if the concentration of NO_x in the headspace is an issue. Potential chemical incompatibility issues with the 72B shipping cask, with other wastes, the WIPP repository backfill, and the repository seal and panel closure materials need to be investigated. It is also unclear whether waste form off-gassing will exceed limits established at WIPP with respect to worker safety.

6. RECOMMENDATIONS

- Tests should be completed with actual SBW or with a simulant that includes minor constituents, such as silicates and carbonates, that may contribute to fouling.
- Hydrogen gas generation testing on bottoms product produced from real waste or simulated waste with a representative concentration of plutonium is necessary to validate that the final waste form is WIPP-shippable in the 72B cask.
- Cesium appears to be non-volatile at the evaporation temperatures used for these experiments, based on analysis of the overheads condensate. However, the cesium was below detection limits and additional tests with higher cesium concentrations would confirm this conclusion.
- Additional evaluation should be performed to determine if the concentration of NO_x in the headspace of the bottoms containers is an issue. This evaluation must include (1) identification of acceptable NO_x concentrations for shipment and disposal and (2) testing to determine (a) a waste canister stabilization period or (b) engineered solutions to mitigate the NO_x concentrations.
- The cooling dynamics of a full-scale container of bottoms product should be modeled. The cooling curves already generated from these tests could be used; however, additional experimental data are necessary to accurately measure the parameters required for the model. The data generated from the model would be useful in feasibility studies and cost estimates for a production-scale E/S process.
- Full-scale testing is recommended primarily to verify that the bottoms discharge system is reliable when designing the production facility. It should not be assumed that components such as valves, piping, or pumps would function reliably with a hot, viscous bottoms product material whose properties change readily with temperature, concentration, and time.

7. REFERENCES

1. R. J. Kirkham, Lockheed Martin Idaho Technologies Company, to W. H. Landman, "Sodium Bearing Waste Solidification by Evaporation," RJK-6-98, September 29, 1998.
2. J. A. McCray, L. G. Olson, S. J. Losinski, *Investigation of Direct Evaporation and Fractional Crystallization Technologies for Sodium-Bearing Waste Treatment*, INEEL/EXT-02-01043, Idaho National Engineering and Environmental Laboratory, September 2002.
3. R. J. Kirkham, et. al., *Direct Evaporation of Sodium-Bearing Waste: Flask-Scale Testing of WM-189 Simulant*, INEEL/EXT-03-00657, Idaho National Engineering and Environmental Laboratory, June 2003.
4. EDF-3443, "Preliminary Assessment of Evaporator Technologies for Direct Evaporation of Sodium-Bearing Waste," E. B. Packer, Idaho National Engineering and Environmental Laboratory, April 8, 2003.
5. D. L. Griffith, S. J. Losinski, B. E. Olaveson, and L. G. Olson, *Testing an Agitated Thin Film Evaporator for Solidifying Simulated Sodium-Bearing Waste-Test Series 1*, INEEL/EXT-03-00680, June 2003.
6. D. L. Griffith, L. G. Olson, *Testing an Agitated Thin Film Evaporator for Solidifying a Mixture of Simulated Sodium-Bearing Waste and Undissolved Solids (Test Series 2)*, INEEL/EXT-03-01189, Idaho National Engineering and Environmental Laboratory, November 2003.
7. EDF-2373, "Process Design of SBW Treatment Alternatives," C. M. Barnes, Idaho National Engineering and Environmental Laboratory, September 10, 2002.
8. W. D. St. Michel, R. E. Arbon, Bechtel BWXT Idaho, LLC, "RH-TRU Waste Form Development and Carlsbad Field Office/Waste Isolation Pilot Plant Evaluation Parameters," WDS-01-03 & REA-01-03, October 16, 2003.
9. EDF-3679, "Direct Evaporation Process Design," C. M. Barnes, R. W. Wood, Idaho National Engineering and Environmental Laboratory, September 10, 2003.
10. EDF-3392, "Radiolytic Hydrogen Gas Generation in Dried SBW UDS and Tank Solids," D. S., Wendt, Idaho National Engineering and Environmental Laboratory, February 26, 2002.
11. D. L. Griffith, "Test Plan for Evaporation/Solidification of SBW Simulant Using an Agitated Thin-Film Evaporator with Heel Solids Simulant," INEEL Project 22681, TFP-77-03, June 16, 2000.
12. J. D. Christian, *Composition and Simulation of Tank WM-180 Sodium-Bearing Waste at the Idaho Nuclear Technology and Engineering Center*, INEEL/EXT-2001-00600, Idaho National Engineering and Environmental Laboratory, May 2001.

APPENDIX A

Analytical Results for Feed and Distillate Composition

Appendix A

Analytical Results for Feed and Distillate Composition

Reported data from the Analytical Laboratory.

Log #	Index	Field Sample Name	ALD Lab ID	Method #	Analyte	Result String	Result	Standard Deviation	Units
031209-2	45	AL-1 Feed	3CE64	7012	ACID	1.97E+00 +- 1.6E-01 Normal Acid	1.9721579	0.1620796	Normal Acid
031209-2	21	AL-1 Feed	3CE64	2900	ALUMINUM	3.69582E+04 ug/ml	36958.223	0	ug/ml
031209-2	21	AL-1 Feed	3CE64	2900	CALCIUM	2.22826E+03 ug/ml	2228.262	0	ug/ml
031209-2	9	AL-1 Feed	3CE64	2111	CESIUM	40.2 ug/mL			
031209-2	33	AL-1 Feed	3CE64	8100	FLUORIDE	< 6.0004E-01 mg/L	0.60004	0	mg/L
031209-2	21	AL-1 Feed	3CE64	2900	IRON	1.21687E+03 ug/ml	1216.8695	0	ug/ml
031209-2	21	AL-1 Feed	3CE64	2900	MAGNESIUM	4.44804E+02 ug/ml	444.804	0	ug/ml
031209-2	21	AL-1 Feed	3CE64	2900	MANGANESE	8.99304E+02 ug/ml	899.304	0	ug/ml
031209-2	33	AL-1 Feed	3CE64	8100	NITRATE	3.09342E+05 mg/L	309341.57	0	mg/L
031209-2	21	AL-1 Feed	3CE64	2900	POTASSIUM	6.52844E+03 ug/ml	6528.438	0	ug/ml
031209-2	21	AL-1 Feed	3CE64	2900	SODIUM	3.79273E+04 ug/ml	37927.318	0	ug/ml
031209-2	33	AL-1 Feed	3CE64	8100	SULFATE	5.72895E+03 mg/L	5728.9515	0	mg/L
031209-2	21	AL-1 Feed	3CE64	2900	SULFUR	2.88244E+03 ug/ml	2882.439	0	ug/ml
031209-2	46	AL-2 Feed	3CE65	7012	ACID	1.93E+00 +- 1.6E-01 Normal Acid	1.9288668	0.1604987	Normal Acid
031209-2	22	AL-2 Feed	3CE65	2900	ALUMINUM	3.34185E+04 ug/ml	33418.476	0	ug/ml
031209-2	22	AL-2 Feed	3CE65	2900	CALCIUM	2.03919E+03 ug/ml	2039.19	0	ug/ml
031209-2	10	AL-2 Feed	3CE65	2111	CESIUM	24.3 ug/mL			
031209-2	34	AL-2 Feed	3CE65	8100	FLUORIDE	< 6.0004E-01 mg/L	0.60004	0	mg/L
031209-2	22	AL-2 Feed	3CE65	2900	IRON	1.08632E+03 ug/ml	1086.3197	0	ug/ml
031209-2	22	AL-2 Feed	3CE65	2900	MAGNESIUM	4.0703E+02 ug/ml	407.03	0	ug/ml
031209-2	22	AL-2 Feed	3CE65	2900	MANGANESE	7.95072E+02 ug/ml	795.072	0	ug/ml
031209-2	34	AL-2 Feed	3CE65	8100	NITRATE	3.11968E+05 mg/L	311967.72	0	mg/L
031209-2	22	AL-2 Feed	3CE65	2900	POTASSIUM	5.75852E+03 ug/ml	5758.515	0	ug/ml
031209-2	22	AL-2 Feed	3CE65	2900	SODIUM	3.27656E+04 ug/ml	32765.612	0	ug/ml
031209-2	34	AL-2 Feed	3CE65	8100	SULFATE	5.70776E+03 mg/L	5707.7625	0	mg/L
031209-2	22	AL-2 Feed	3CE65	2900	SULFUR	2.86547E+03 ug/ml	2865.471	0	ug/ml
031209-2	47	MG-1 Feed	3CE66	7012	ACID	1.84E+00 +- 1.6E-01 Normal Acid	1.837907	0.1571269	Normal Acid
031209-2	23	MG-1 Feed	3CE66	2900	ALUMINUM	1.47812E+04 ug/ml	14781.249	0	ug/ml
031209-2	23	MG-1 Feed	3CE66	2900	CALCIUM	2.27068E+03 ug/ml	2270.682	0	ug/ml
031209-2	11	MG-1 Feed	3CE66	2111	CESIUM	26.7 ug/mL			
031209-2	35	MG-1 Feed	3CE66	8100	FLUORIDE	< 6.0004E-01 mg/L	0.60004	0	mg/L
031209-2	23	MG-1 Feed	3CE66	2900	IRON	1.25503E+03 ug/ml	1255.026	0	ug/ml
031209-2	23	MG-1 Feed	3CE66	2900	MAGNESIUM	2.34011E+04 ug/ml	23401.094	0	ug/ml

Log #	Index	Field Sample Name	ALD Lab ID	Method #	Analyte	Result String	Result	Standard Deviation	Units
031209-2	23	MG-1 Feed	3CE66	2900	MANGANESE	8.06586E+02 ug/ml	806.586	0	ug/ml
031209-2	35	MG-1 Feed	3CE66	8100	NITRATE	3.06059E+05 mg/L	306059	0	mg/L
031209-2	23	MG-1 Feed	3CE66	2900	POTASSIUM	7.5041E+03 ug/ml	7504.098	0	ug/ml
031209-2	23	MG-1 Feed	3CE66	2900	SODIUM	3.88046E+04 ug/ml	38804.604	0	ug/ml
031209-2	35	MG-1 Feed	3CE66	8100	SULFATE	5.7784E+03 mg/L	5778.4002	0	mg/L
031209-2	23	MG-1 Feed	3CE66	2900	SULFUR	2.92062E+03 ug/ml	2920.617	0	ug/ml
031209-2	48	MG-2 Feed	3CE67	7012	ACID	2.10E+00 +- 1.7E-01 Normal Acid	2.1010582	0.1667006	Normal Acid
031209-2	24	MG-2 Feed	3CE67	2900	ALUMINUM	1.44956E+04 ug/ml	14495.621	0	ug/ml
031209-2	24	MG-2 Feed	3CE67	2900	CALCIUM	2.22099E+03 ug/ml	2220.99	0	ug/ml
031209-2	12	MG-2 Feed	3CE67	2111	CESIUM	26.3 ug/mL			
031209-2	36	MG-2 Feed	3CE67	8100	FLUORIDE	< 6.0004E-01 mg/L	0.60004	0	mg/L
031209-2	24	MG-2 Feed	3CE67	2900	IRON	1.23503E+03 ug/ml	1235.028	0	ug/ml
031209-2	24	MG-2 Feed	3CE67	2900	MAGNESIUM	2.33909E+04 ug/ml	23390.893	0	ug/ml
031209-2	24	MG-2 Feed	3CE67	2900	MANGANESE	7.9992E+02 ug/ml	799.92	0	ug/ml
031209-2	36	MG-2 Feed	3CE67	8100	NITRATE	3.06716E+05 mg/L	306715.5	0	mg/L
031209-2	24	MG-2 Feed	3CE67	2900	POTASSIUM	7.52743E+03 ug/ml	7527.429	0	ug/ml
031209-2	24	MG-2 Feed	3CE67	2900	SODIUM	3.80905E+04 ug/ml	38090.534	0	ug/ml
031209-2	36	MG-2 Feed	3CE67	8100	SULFATE	4.82158E+03 mg/L	4821.5788	0	mg/L
031209-2	24	MG-2 Feed	3CE67	2900	SULFUR	3.03727E+03 ug/ml	3037.272	0	ug/ml
031209-2	37	AL-1-1	3CE56	7012	ACID	3.22E+00 +- 2.0E-01 Normal Acid	3.2241934	0.2026907	Normal Acid
031209-2	13	AL-1-1	3CE56	2900	ALUMINUM	1.9728E+00 ug/ml	1.9728	0	ug/ml
031209-2	13	AL-1-1	3CE56	2900	CALCIUM	1.7424E+00 ug/ml	1.7424	0	ug/ml
031209-2	1	AL-1-1	3CE56	2111	CESIUM	<0.00505 ug/mL			
031209-2	25	AL-1-1	3CE56	8100	FLUORIDE	< 6.0004E-01 mg/L	0.60004	0	mg/L
031209-2	13	AL-1-1	3CE56	2900	IRON	4.7382E+00 ug/ml	4.7382	0	ug/ml
031209-2	13	AL-1-1	3CE56	2900	MAGNESIUM	1.4724E+00 ug/ml	1.4724	0	ug/ml
031209-2	13	AL-1-1	3CE56	2900	MANGANESE	1.32E-01 ug/ml	0.132	0	ug/ml
031209-2	25	AL-1-1	3CE56	8100	NITRATE	1.5652E+05 mg/L	156519.96	0	mg/L
031209-2	13	AL-1-1	3CE56	2900	POTASSIUM	Not Detected: IDL= 0.2964 ug/ml	0.2964	0	ug/ml
031209-2	13	AL-1-1	3CE56	2900	SODIUM	1.8426E+00 ug/ml	1.8426	0	ug/ml
031209-2	25	AL-1-1	3CE56	8100	SULFATE	< 1.18996E+01 mg/L	11.89961	0	mg/L
031209-2	13	AL-1-1	3CE56	2900	SULFUR	3.942E-01 ug/ml	0.3942	0	ug/ml
031209-2	38	AL-1-2	3CE57	7012	ACID	3.26E+00 +- 2.0E-01 Normal Acid	3.2597018	0.203729	Normal Acid
031209-2	14	AL-1-2	3CE57	2900	ALUMINUM	1.785E+00 ug/ml	1.785	0	ug/ml
031209-2	14	AL-1-2	3CE57	2900	CALCIUM	4.566E-01 ug/ml	0.4566	0	ug/ml
031209-2	2	AL-1-2	3CE57	2111	CESIUM	<0.00505 ug/mL			
031209-2	26	AL-1-2	3CE57	8100	FLUORIDE	< 6.0004E-01 mg/L	0.60004	0	mg/L

Log #	Index	Field Sample Name	ALD Lab ID	Method #	Analyte	Result String	Result	Standard Deviation	Units
031209-2	14	AL-1-2	3CE57	2900	IRON	3.8058E+00 ug/ml	3.8058	0	ug/ml
031209-2	14	AL-1-2	3CE57	2900	MAGNESIUM	5.826E-01 ug/ml	0.5826	0	ug/ml
031209-2	14	AL-1-2	3CE57	2900	MANGANESE	1.02E-01 ug/ml	0.102	0	ug/ml
031209-2	26	AL-1-2	3CE57	8100	NITRATE	1.31625E+05 mg/L	131624.58	0	mg/L
031209-2	14	AL-1-2	3CE57	2900	POTASSIUM	Not Detected: IDL= 0.2964 ug/ml	0.2964	0	ug/ml
031209-2	14	AL-1-2	3CE57	2900	SODIUM	1.809E+00 ug/ml	1.809	0	ug/ml
031209-2	26	AL-1-2	3CE57	8100	SULFATE	< 1.18996E+01 mg/L	11.89961	0	mg/L
031209-2	14	AL-1-2	3CE57	2900	SULFUR	2.934E-01 ug/ml	0.2934	0	ug/ml
031209-2	39	AL-2-1	3CE58	7012	ACID	3.99E+00 +- 2.2E-01 Normal Acid	3.9873806	0.2239984	Normal Acid
031209-2	15	AL-2-1	3CE58	2900	ALUMINUM	1.6176E+00 ug/ml	1.6176	0	ug/ml
031209-2	15	AL-2-1	3CE58	2900	CALCIUM	2.724E-01 ug/ml	0.2724	0	ug/ml
031209-2	3	AL-2-1	3CE58	2111	CESIUM	<0.00505 ug/mL			
031209-2	27	AL-2-1	3CE58	8100	FLUORIDE	< 6.0004E-01 mg/L	0.60004	0	mg/L
031209-2	15	AL-2-1	3CE58	2900	IRON	5.2086E+00 ug/ml	5.2086	0	ug/ml
031209-2	15	AL-2-1	3CE58	2900	MAGNESIUM	5.934E-01 ug/ml	0.5934	0	ug/ml
031209-2	15	AL-2-1	3CE58	2900	MANGANESE	1.05E-01 ug/ml	0.105	0	ug/ml
031209-2	27	AL-2-1	3CE58	8100	NITRATE	1.49968E+05 mg/L	149967.77	0	mg/L
031209-2	15	AL-2-1	3CE58	2900	POTASSIUM	3.672E-01 ug/ml	0.3672	0	ug/ml
031209-2	15	AL-2-1	3CE58	2900	SODIUM	1.5642E+00 ug/ml	1.5642	0	ug/ml
031209-2	27	AL-2-1	3CE58	8100	SULFATE	< 1.18996E+01 mg/L	11.89961	0	mg/L
031209-2	15	AL-2-1	3CE58	2900	SULFUR	2.184E-01 ug/ml	0.2184	0	ug/ml
031209-2	40	AL-2-2	3CE59	7012	ACID	4.04E+00 +- 2.3E-01 Normal Acid	4.0433184	0.2254851	Normal Acid
031209-2	16	AL-2-2	3CE59	2900	ALUMINUM	2.1534E+00 ug/ml	2.1534	0	ug/ml
031209-2	16	AL-2-2	3CE59	2900	CALCIUM	3.6E-01 ug/ml	0.36	0	ug/ml
031209-2	4	AL-2-2	3CE59	2111	CESIUM	<0.00505 ug/mL			
031209-2	28	AL-2-2	3CE59	8100	FLUORIDE	< 6.0004E-01 mg/L	0.60004	0	mg/L
031209-2	16	AL-2-2	3CE59	2900	IRON	6.936E+00 ug/ml	6.936	0	ug/ml
031209-2	16	AL-2-2	3CE59	2900	MAGNESIUM	7.836E-01 ug/ml	0.7836	0	ug/ml
031209-2	16	AL-2-2	3CE59	2900	MANGANESE	1.56E-01 ug/ml	0.156	0	ug/ml
031209-2	28	AL-2-2	3CE59	8100	NITRATE	1.52589E+05 mg/L	152588.58	0	mg/L
031209-2	16	AL-2-2	3CE59	2900	POTASSIUM	Not Detected: IDL= 0.2964 ug/ml	0.2964	0	ug/ml
031209-2	16	AL-2-2	3CE59	2900	SODIUM	1.9596E+00 ug/ml	1.9596	0	ug/ml
031209-2	28	AL-2-2	3CE59	8100	SULFATE	< 1.18996E+01 mg/L	11.89961	0	mg/L
031209-2	16	AL-2-2	3CE59	2900	SULFUR	2.418E-01 ug/ml	0.2418	0	ug/ml
031209-2	41	MG-1-1	3CE60	7012	ACID	3.62E+00 +- 2.1E-01 Normal Acid	3.624514	0.2141183	Normal Acid
031209-2	17	MG-1-1	3CE60	2900	ALUMINUM	4.7904E+00 ug/ml	4.7904	0	ug/ml

Log #	Index	Field Sample Name	ALD Lab ID	Method #	Analyte	Result String	Result	Standard Deviation	Units
031209-2	17	MG-1-1	3CE60	2900	CALCIUM	1.8606E+00 ug/ml	1.8606	0	ug/ml
031209-2	5	MG-1-1	3CE60	2111	CESIUM	<0.00505 ug/mL			
031209-2	29	MG-1-1	3CE60	8100	FLUORIDE	< 6.0004E-01 mg/L	0.60004	0	mg/L
031209-2	17	MG-1-1	3CE60	2900	IRON	2.0274E+01 ug/ml	20.274	0	ug/ml
031209-2	17	MG-1-1	3CE60	2900	MAGNESIUM	4.6242E+00 ug/ml	4.6242	0	ug/ml
031209-2	17	MG-1-1	3CE60	2900	MANGANESE	3.504E-01 ug/ml	0.3504	0	ug/ml
031209-2	29	MG-1-1	3CE60	8100	NITRATE	1.35555E+05 mg/L	135554.9	0	mg/L
031209-2	17	MG-1-1	3CE60	2900	POTASSIUM	2.0964E+00 ug/ml	2.0964	0	ug/ml
031209-2	17	MG-1-1	3CE60	2900	SODIUM	8.706E+00 ug/ml	8.706	0	ug/ml
031209-2	29	MG-1-1	3CE60	8100	SULFATE	< 1.18996E+01 mg/L	11.89961	0	mg/L
031209-2	17	MG-1-1	3CE60	2900	SULFUR	8.766E-01 ug/ml	0.8766	0	ug/ml
031209-2	42	MG-1-2	3CE61	7012	ACID	3.30E+00 +- 2.0E-01 Normal Acid	3.2995879	0.2048893	Normal Acid
031209-2	18	MG-1-2	3CE61	2900	ALUMINUM	1.3722E+00 ug/ml	1.3722	0	ug/ml
031209-2	18	MG-1-2	3CE61	2900	CALCIUM	4.98E-01 ug/ml	0.498	0	ug/ml
031209-2	6	MG-1-2	3CE61	2111	CESIUM	<0.00505 ug/mL			
031209-2	30	MG-1-2	3CE61	8100	FLUORIDE	< 6.0004E-01 mg/L	0.60004	0	mg/L
031209-2	18	MG-1-2	3CE61	2900	IRON	5.3556E+00 ug/ml	5.3556	0	ug/ml
031209-2	18	MG-1-2	3CE61	2900	MAGNESIUM	2.6226E+00 ug/ml	2.6226	0	ug/ml
031209-2	18	MG-1-2	3CE61	2900	MANGANESE	1.746E-01 ug/ml	0.1746	0	ug/ml
031209-2	30	MG-1-2	3CE61	8100	NITRATE	1.12631E+05 mg/L	112630.82	0	mg/L
031209-2	18	MG-1-2	3CE61	2900	POTASSIUM	5.556E-01 ug/ml	0.5556	0	ug/ml
031209-2	18	MG-1-2	3CE61	2900	SODIUM	3.1224E+00 ug/ml	3.1224	0	ug/ml
031209-2	30	MG-1-2	3CE61	8100	SULFATE	< 1.18996E+01 mg/L	11.89961	0	mg/L
031209-2	18	MG-1-2	3CE61	2900	SULFUR	2.658E-01 ug/ml	0.2658	0	ug/ml
031209-2	43	MG-2-1	3CE62	7012	ACID	3.79E+00 +- 2.2E-01 Normal Acid	3.7942733	0.2187931	Normal Acid
031209-2	19	MG-2-1	3CE62	2900	ALUMINUM	1.5168E+00 ug/ml	1.5168	0	ug/ml
031209-2	19	MG-2-1	3CE62	2900	CALCIUM	5.418E-01 ug/ml	0.5418	0	ug/ml
031209-2	7	MG-2-1	3CE62	2111	CESIUM	<0.00505 ug/mL			
031209-2	31	MG-2-1	3CE62	8100	FLUORIDE	< 6.0004E-01 mg/L	0.60004	0	mg/L
031209-2	19	MG-2-1	3CE62	2900	IRON	4.2786E+00 ug/ml	4.2786	0	ug/ml
031209-2	19	MG-2-1	3CE62	2900	MAGNESIUM	2.625E+00 ug/ml	2.625	0	ug/ml
031209-2	19	MG-2-1	3CE62	2900	MANGANESE	1.332E-01 ug/ml	0.1332	0	ug/ml
031209-2	31	MG-2-1	3CE62	8100	NITRATE	1.53244E+05 mg/L	153243.8	0	mg/L
031209-2	19	MG-2-1	3CE62	2900	POTASSIUM	7.806E-01 ug/ml	0.7806	0	ug/ml
031209-2	19	MG-2-1	3CE62	2900	SODIUM	3.8094E+00 ug/ml	3.8094	0	ug/ml
031209-2	31	MG-2-1	3CE62	8100	SULFATE	< 1.18996E+01 mg/L	11.89961	0	mg/L
031209-2	19	MG-2-1	3CE62	2900	SULFUR	3.078E-01 ug/ml	0.3078	0	ug/ml

Log #	Index	Field Sample Name	ALD Lab ID	Method #	Analyte	Result String	Result	Standard Deviation	Units
031209-2	44	MG-2-2	3CE63	7012	ACID	3.88E+00 +- 2.2E-01 Normal Acid	3.8828011	0.2211938	Normal Acid
031209-2	20	MG-2-2	3CE63	2900	ALUMINUM	1.3074E+00 ug/ml	1.3074	0	ug/ml
031209-2	20	MG-2-2	3CE63	2900	CALCIUM	4.86E-01 ug/ml	0.486	0	ug/ml
031209-2	8	MG-2-2	3CE63	2111	CESIUM	<0.00505 ug/mL			
031209-2	32	MG-2-2	3CE63	8100	FLUORIDE	< 6.0004E-01 mg/L	0.60004	0	mg/L
031209-2	20	MG-2-2	3CE63	2900	IRON	5.6022E+00 ug/ml	5.6022	0	ug/ml
031209-2	20	MG-2-2	3CE63	2900	MAGNESIUM	2.6634E+00 ug/ml	2.6634	0	ug/ml
031209-2	20	MG-2-2	3CE63	2900	MANGANESE	1.704E-01 ug/ml	0.1704	0	ug/ml
031209-2	32	MG-2-2	3CE63	8100	NITRATE	1.5783E+05 mg/L	157830.46	0	mg/L
031209-2	20	MG-2-2	3CE63	2900	POTASSIUM	5.376E-01 ug/ml	0.5376	0	ug/ml
031209-2	20	MG-2-2	3CE63	2900	SODIUM	3.1536E+00 ug/ml	3.1536	0	ug/ml
031209-2	32	MG-2-2	3CE63	8100	SULFATE	< 1.18996E+01 mg/L	11.89961	0	mg/L
031209-2	20	MG-2-2	3CE63	2900	SULFUR	3.09E-01 ug/ml	0.309	0	ug/ml